

Construction and local equivalence of dual-unitary operators: from dynamical maps to quantum combinatorial designs

Suhail Ahmad Rather,^{1,*} S. Aravinda,^{2,†} and Arul Lakshminarayanan¹

¹*Department of Physics, Indian Institute of Technology Madras, Chennai, India 600036*

²*Department of Physics, Indian Institute of Technology Tirupati, Tirupati, India 517619*

While quantum circuits built from two-particle dual-unitary (maximally entangled) operators serve as minimal models of typically nonintegrable many-body systems, the construction and characterization of dual-unitary operators themselves are only partially understood. A nonlinear map on the space of unitary operators was proposed in PRL. 125, 070501 (2020) that results in operators being arbitrarily close to dual unitaries. Here we study the map analytically for the two-qubit case describing the basins of attraction, fixed points, and rates of approach to dual unitaries. A subset of dual-unitary operators having maximum entangling power are 2-unitary operators or perfect tensors, and are equivalent to four-party absolutely maximally entangled states. It is known that they only exist if the local dimension is larger than $d = 2$. We use the nonlinear map, and introduce stochastic variants of it, to construct explicit examples of new dual and 2-unitary operators. A necessary criterion for their local unitary equivalence to distinguish classes is also introduced and used to display various concrete results and some conjectures. It is known that orthogonal Latin squares provide a “classical combinatorial design” for constructing permutations that are 2-unitary. We extend the underlying design from classical to genuine quantum ones for general dual-unitary operators and give an example of what might be the smallest sized genuinely quantum design of a 2-unitary in $d = 4$.

CONTENTS

I. Introduction	2	V. Combinatorial designs corresponding to dual unitary operators	14
II. Preliminaries and definitions	4	A. Permutation matrices: classical design	14
A. Operator entanglement and entangling power	4	B. General dual-unitary operators: Quantum design	14
B. Matrix reshaping	4	C. Combinatorial structures of known families of dual unitaries	16
III. Dual-unitary and 2-unitary operators from nonlinear iterative maps	5	1. Diagonal ensemble	16
A. Dynamical map for dual unitaries	5	2. Block-diagonal ensemble	16
1. Dual unitaries as fixed points	6		
B. Dynamical map for 2-unitaries	6	VI. Local unitary equivalence of 2-unitary operators	17
1. 2-unitaries as fixed points	7	A. A necessary criterion	17
C. Structured dual unitaries from stochastic maps	7	B. 2-unitaries in $d = 3$	17
IV. Dynamical map in the two-qubit case	8	1. Permutations	17
A. \mathcal{M}_R map in the Weyl chamber	8	2. LU equivalence of 2-unitaries in $d = 3$	18
B. Deriving the map for special initial conditions	10	C. 2-unitaries in $d = 4$	18
1. XY family: plane $c_3 = 0$	10	1. Permutations	18
2. XXX family: $c_1 = c_2 = c_3$	10	2. Entangled OLS of size 4: A new example of AME(4,4)	19
3. SWAP-CNOT-DCNOT face; $c_1^{(0)} = \pi/4$	11	VII. Entangling properties of dual and T-dual permutation matrices	20
4. SWAP-CNOT edge	12	A. Dual-unitary and T-dual permutations in $d = 2$ and $d = 3$	20
5. XXZ family: $c_1 = c_2$	12	B. Numerical results for $d > 3$	22
6. Generic initial conditions	13		
VIII. Summary and discussions	23		
Acknowledgments	24		
References	24		

* suhailmushtaq@physics.iitm.ac.in

† aravinda@iitp.ac.in

A. Details about the map in the two-qubit case	26
B. Details about the map in terms of Cartan parameters	28
1. Map in terms of Cartan parameters	28
a. XXX family	28
b. SWAP-CNOT-DCNOT face	28
c. SWAP-CNOT edge	29
C. 2-unitaries with entangled rows and columns	29

I. INTRODUCTION

In recent years a major research trend uses tools of quantum information theory to understand the puzzles of quantum many-body physics. The typically complex entanglement structure of many-body states drives cross fertilization across various fields of research in physics. Particularly, in the areas of condensed matter physics and string theory, quantum information theory continues to play an exciting role in creating new avenues of understanding [1–4].

Quantum computers allow the realization of the vision of Feynman [5] on the efficient simulation of physical systems [6]. In the present era of Noisy-Intermediate-Scale-Quantum (NISQ) [7] computing such simulations become realistic [8]. The universality of quantum computing allows simulation of any quantum system, where quantum circuits are built using unitary operators or gates acting on single particle and two particle subsystems. A quantum computer is itself a controllable quantum many-body system. Traditional approaches involve studying the properties of systems based on the Hamiltonian evolution and spectra. At this juncture it is important to understand properties of quantum many-body systems from the quantum circuit formalism and to contrast that with the traditional studies.

Quantum advantage using random unitary circuits has been explored in recent experiments using Google’s “sycamore” processor [9] and “Zuchongzhi 2.0” [10]. Similar models are used in studies of entanglement evolution in many-body quantum systems in which the random unitary gates operate on two-body subsystems [11–15]. Quantum circuits, in arbitrary local dimensions, without any random interactions have been proposed as elegant minimal models that can span the gamut of integrable to fully chaotic quantum many-body systems [16–19]. These quantum circuits have a special “duality” property that the evolution operator in the spatial as well as in the temporal direction of the circuit are governed by unitary dynamics. The origin of the duality lies in the two-particle interaction from which the many-body circuits are built, these being *dual-unitary* operators [17]. This duality facilitates an analytical

treatment of many quantities such as two-point correlation functions, spectral form-factors, operator entanglement, out-of-time-order correlators and the exact study of the entanglement dynamics [17, 18, 20–35]. The two-particle unitary from which the circuit is built, plays a significant role in the following and is an operator in d^2 dimensional space where the local dimension is d and is typically denoted as U .

On the other hand entanglement of unitary operators, similar to states, has been studied from the early days of quantum information theory [36–45]. Quantities such as operator entanglement [37], entangling power [36] and complexity of an operator [46] are few measures that quantify the nonlocal properties of unitary operators. Operator entanglement measures how entangled an operator is when viewed as a vector in a product vector space. It has been identified that an unitary operator is dual-unitary if and only if it has maximum possible operator entanglement [47]. Entangling power quantifies the average entanglement produced by a bipartite unitary operator acting on an ensemble of pure product states. A special subclass of dual-unitary operators are those having the maximum possible entangling power allowed by local dimensions. These are the same operators that have been referred to variously as 2-unitary [48] or perfect tensors [49].

The exactly calculable two-point correlation functions in dual-unitary circuits enables the characterization of the many-body system in terms of an ergodic hierarchy, from ergodic to Bernoulli through mixing [17, 50]. It is identified that the dual-unitary circuit is Bernoulli, when correlations instantly decay, if and only if the two-particle unitary operator has maximum entangling power [50]. Additionally, a sufficient condition for the many-body circuit to show the mixing behavior is derived as a function of entangling power [50]. These results establish a close connection between the entangling properties of two particle unitary operators from which the many-body quantum circuits are built and the dynamical nature of the many-body systems.

Let a bipartite pure quantum state’s Schmidt form be $|\psi\rangle_{AB} = \sum_{i=0}^{d-1} \sqrt{\lambda_i} |ii\rangle / \sqrt{d}$, where d is the local Hilbert space dimension. Setting $\lambda_i = 1$ for all i in this expansion results in $|\Phi\rangle = \sum_{i=1}^d |ii\rangle / \sqrt{d}$ which is a maximally entangled state, in fact the one that is closest to $|\psi_{AB}\rangle$. Any set of orthonormal bases in the subspaces constructs such maximally entangled states.

In contrast the construction of maximally entangled unitary operators do not follow from orthonormal operator bases. Express an unitary operator in operator Schmidt form, $U = \sum_{j=1}^{d^2} \sqrt{\lambda_j} X_j \otimes Y_j$, $\text{tr}(X_j X_k) = \text{tr}(Y_j Y_k) = \delta_{jk}$ and $\lambda_j \geq 0$. U is maximally entangled or dual-unitary iff $\lambda_i = 1$ for all i . However the constraint of unitarity is more stronger than the constraint

of normalization on the state and this imposes complex conditions on the Schmidt matrices X_j and Y_j . Thus simply assigning $\lambda_i = 1$ for all i does not retain unitarity although it does result in a maximally entangled (in general nonunitary) operator. This makes it hard to analytically construct dual-unitary operators.

If the local dimension is $d = 2$, namely for qubits, all possible dual-unitary operators can be parametrized using the Cartan decomposition [17]. There are no 2-unitary or perfect tensors in this case. While a complete parametrization of dual-unitary operators for $d > 2$ is not known, many classes and examples have been examined and used thus far. The SWAP or flip operator is a simple example of a dual-unitary operator. The discrete Fourier transform in d^2 dimensions maximizes operator entanglement [51, 52] and is hence also a dual-unitary. However, the SWAP has zero entangling power, while the Fourier transform has a finite value. Diagonal and block diagonal operators, along with the SWAP gate can be used to construct dual-unitary operator [50, 53]. These have limited entangling power and in particular cannot reach the maximum value [50]. The dual-unitary operators introduced recently in Ref. [54] are also bounded by the entangling power of diagonal unitary operators.

A numerical iterative algorithm which produces unitary operators arbitrarily close to being dual-unitary has been presented in [47]. This algorithm can yield dual-unitary operators with a wide range of entangling powers, especially exceeding the bound corresponding to block-diagonal based constructions. Remarkably, the numerical algorithm can also yield exact analytical forms for dual-unitary operators [50] and several other examples, including new 2-unitaries, are displayed further below. A slightly modified algorithm has been used to positively settle an open problem on the existence of four-party absolutely maximally entangled (AME) states of local dimension six [55], see also Ref. [56] for an elaborate discussion of the solution. AME states are genuinely entangled multipartite pure states which have maximal entanglement in all bipartitions [57]. Thus an AME state of N qudits each of dimension d denoted as $\text{AME}(N, d)$ has all subsystems of size $\lfloor N/2 \rfloor$ maximally mixed.

The numerical algorithm acts generically as a dynamical map in the space of unitary operators. These are thus high dimensional dynamical systems which deserve to be studied in their own right. In this work, we study the fixed point structure of the map. In particular for the case of two qubits, an explicit analytical form of the map is derived. This enables deriving dynamical characteristics such as the rate of approach to attractors which are dual-unitary operators. A variety of dynamical behaviours have been observed: (i) power-law approaches to the SWAP gate, (ii) exponential approach to

other dual unitary gates, with a rate that diverges for the maximally entangling case of the DCNOT gate.

Due to operator-state isomorphism, a 2-unitary operator is equivalent to a four-party AME state [48]. There are various ways of constructing AME states in which quantum combinatorial designs are used [48, 58]. Since 2-unitaries are a subset of dual unitaries, a less restrictive combinatorial design underlying dual-unitary operators that are permutations was found in [50]. In this work, we extend such combinatorial designs to dual-unitary operators going beyond permutations. We define *stochastic* dynamical maps capable of generating such structured dual-unitary operators.

Apart from dual-unitary operators, the maps presented in [47] can be used to generate infinitely many 2-unitaries for $d > 2$. An important question now arises if the 2-unitaries so obtained are local unitarily (LU) equivalent to each other and to 2-unitary permutations of the same size. Two bipartite unitary operators U and U' on $\mathcal{H}_d \otimes \mathcal{H}_d$ are said to local unitarily equivalent, denoted $U \xrightarrow{\text{LU}} U'$, if there exist single qudit unitary gates u_1, u_2, v_1, v_2 such that

$$U' = (u_1 \otimes u_2)U(v_1 \otimes v_2). \quad (1)$$

However, as far as we know, there is no general procedure to identify LU equivalent unitary operators, apart from the case of two-qubits [45]. This problem becomes acute when the operators concerned have the same entangling powers, such as the 2-unitaries. In this work, we address this question by proposing a necessary criterion for LU equivalence between bipartite unitary operators that can potentially work also in the case of 2-unitaries.

This leads us to conjecture that *all* two-qutrit 2-unitaries are LU equivalent to each other. From an exhaustive search, we find that the special subset of 72 possible 2-unitary permutations of size 9 are LU equivalent to each other. For local Hilbert space dimension $d = 4$, we find that this still continues to hold: indeed there are 6912 2-unitary permutations, and we find that these can be generated from any one of them by local permutations. Thus up to LU equivalence, we find that there is *only one* 2-unitary permutation in $d = 3, 4$ and implies that there is only one unique orthogonal Latin square of size 3 and 4. Note that the connection between 2-unitary permutations and orthogonal Latin squares has been known for some time [59].

Although there is only one 2-unitary permutation up to LU equivalence, further below, we give an explicit example of a 2-unitary of size 16 which is not LU equivalent to any 2-unitary permutation of the same size. In other words, we give an explicit example of an AME state of four ququads which is not LU connected to an AME state of four ququads with minimal support. Minimal support four-party AME states have d^2 nonva-

nishing coefficients in some product orthonormal basis, which is the smallest number possible [48]. These new examples of AME states can be used to construct new error-correcting codes as was done in [55] and can provide insights about the most general underlying combinatorial designs 2-unitaries possess. For $d = 5$ we show that there are two LU inequivalent 2-unitary permutations or equivalently, two LU inequivalent AME states of minimal support. This contradicts *Conjecture 2* in Ref. [60] which implies that all four party AME states of minimal support are LU equivalent for all local dimensions d .

The paper is structured as follows. In Sec. (II), the basic terminologies used in the current work is defined. In Sec. (III), the non-linear iterative maps from which dual-unitary and 2-unitary operators are produced is described, and their fixed point structure is discussed. Stochastic generalizations are introduced to result in specially structured operators. In Sec. (IV) the iterative map is studied in explicit forms for the case of qubits. Here we analytically estimate the power-law or exponential approach to dual-unitary operators. In Sec (V) combinatorial designs corresponding to dual-unitary operators is discussed. In Sec. (VI) the question of local unitary equivalence of 2-unitary operators is discussed, specially for the small cases of $d = 3$, and 4. In Sec. (VII) permutations small dimensions is studied in detail via their entangling powers and gate-typicality. Classification of LU classes for dual-unitary and T-dual unitary permutation operators is given for $d = 2, 3$. Finally we conclude in Sec. (VIII).

II. PRELIMINARIES AND DEFINITIONS

In this section, we mostly recall some relevant quantities and measures.

A. Operator entanglement and entangling power

Any operator $X \in \mathcal{H}_d$ is mapped to the state $|X\rangle \in \mathcal{H}_d \otimes \mathcal{H}_d$ as

$$|X\rangle := (X \otimes I) |\Phi\rangle, \quad (2)$$

where $\{|i\rangle\}_{i=1}^d$ is an orthonormal basis in \mathcal{H}_d and $|\Phi\rangle := \frac{1}{\sqrt{d}} \sum_{i=1}^d |ii\rangle$ is the generalized Bell state. A bipartite unitary operator $U = \sum_{ij}^{d^2} \alpha_{ij} e_i^A \otimes e_j^B \in \mathcal{B}(\mathcal{H}_d \otimes \mathcal{H}_d)$, is mapped to $|U\rangle = \sum_{ij}^{d^2} \alpha_{ij} |e_i\rangle_A \otimes |e_j\rangle_B \in \mathcal{H}_{d^2} \otimes \mathcal{H}_{d^2}$, where $e_i^{A,B}$ are a pair of operator bases in \mathcal{H}_d .

The entanglement of an unitary operator U is the entanglement of the state $|U\rangle = \sum_{j=1}^{d^2} \sqrt{\lambda_j} |X_j^A\rangle |Y_j^B\rangle$.

The Schmidt decomposition of U is given by

$$U = \sum_{j=1}^{d^2} \sqrt{\lambda_j} X_j^A \otimes Y_j^B, \quad (3)$$

with $\text{tr}\{X_j^A X_k^A\} = \text{tr}\{Y_j^B Y_k^B\} = \delta_{jk}$, $\sum_{j=1}^{d^2} \lambda_j = d^2$. The *operator entanglement* of U is defined in terms of linear entanglement as

$$E(U) = 1 - \frac{1}{d^4} \sum_{j=1}^{d^2} \lambda_j^2, \quad (4)$$

where $0 \leq E(U) \leq 1 - 1/d^2$.

Another related, but distinct, entanglement facet of an unitary operator U is its *entangling power*, $e_p(U)$. It is defined as the average entanglement produced due to its action on pure product states distributed according to the uniform, Haar measure,

$$e_p(U) = C_d \overline{\mathcal{E}(U |\phi_1\rangle \otimes |\phi_2\rangle)}^{|\phi_1\rangle, |\phi_2\rangle}, \quad (5)$$

where $\mathcal{E}(\cdot)$ can be any entanglement measure, and C_d is a constant scale factor. Considering $\mathcal{E}(\cdot)$ to be the linear entropy, the entangling power can be directly calculated using operator entanglement [37] as follows. Let S be the *swap* operator such that

$$S |\phi_A\rangle |\phi_B\rangle = |\phi_B\rangle |\phi_A\rangle, \quad (6)$$

for all $|\phi_A\rangle \in \mathcal{H}_d$, $|\phi_B\rangle \in \mathcal{H}_d$. We choose C_d such that the scaled entangling power $0 \leq e_p(U) \leq 1$ is given by

$$e_p(U) = \frac{1}{E(S)} [E(U) + E(US) - E(S)], \quad (7)$$

where $E(S) = 1 - 1/d^2$.

Note that the swap operator is such that it has the maximum possible operator entanglement, however the entangling power $e_p(S) = 0$. In fact any operator U and US both share the same entangling power as is clear from Eq. (7). The so-called gate-typicality $g_t(U)$ [61] distinguishes these and is defined as

$$g_t(U) = \frac{1}{2E(S)} [E(U) - E(US) + E(S)], \quad (8)$$

and also ranges from 0 to 1, with $g_t(S) = 1$ and vanishes for all local gates.

B. Matrix reshaping

A bipartite unitary operator U on $\mathcal{H}^d \otimes \mathcal{H}^d$ can be expanded in product basis as

$$U = \sum_{i\alpha j\beta} \langle i\alpha |U|j\beta\rangle |i\alpha\rangle \langle j\beta| \quad (9)$$

There are four basic matrix rearrangements of U that we use in this work :

1. Realignment operations:

$$R_1 : \langle i\alpha|U|j\beta\rangle = \langle\beta\alpha|U^{R_1}|ji\rangle \quad (10)$$

$$R_2 : \langle i\alpha|U|j\beta\rangle = \langle ij|U^{R_2}|\alpha\beta\rangle \quad (11)$$

2. Partial Transpose operations:

$$\Gamma_1 : \langle i\alpha|U|j\beta\rangle = \langle j\alpha|U^{\Gamma_1}|i\beta\rangle \quad (12)$$

$$\Gamma_2 : \langle i\alpha|U|j\beta\rangle = \langle i\beta|U^{\Gamma_2}|j\alpha\rangle \quad (13)$$

The relation between entanglement and matrix reshaping becomes clear on considering the state $|U\rangle$ as now a 4-party state $|\psi\rangle \in \mathcal{H}_d \otimes \mathcal{H}_d \otimes \mathcal{H}_d \otimes \mathcal{H}_d$:

$$|\psi\rangle_{ABCD} = (U_{AB} \otimes I_{CD}) |\Phi\rangle_{AC} |\Phi\rangle_{BD}, \quad (14)$$

where $|\Phi\rangle = \frac{1}{\sqrt{d}} \sum_i^d |ii\rangle$ is the generalized Bell state. The reduced state corresponding to the three possible partition $AB|CD$, $AC|BD$ and $AD|BC$ are given by

$$\rho_{AB} = \frac{1}{d^2} U U^\dagger, \rho_{AC} = \frac{1}{d^2} U^{R_2} U^{R_2\dagger}, \rho_{AD} = \frac{1}{d^2} U^{\Gamma_2} U^{\Gamma_2\dagger}. \quad (15)$$

Using $(X \otimes Y)^{R_2} = |X\rangle\langle Y^*|$, it is easy to see $U^{R_2} U^{R_2\dagger} = \sum_j^{d^2} \lambda_j |X_j\rangle\langle X_j|$. The Schmidt value λ_j are the singular values of U^{R_2} (which are the same as the singular values of U^{R_1}). The operator entanglement $E(U)$ can be interpreted as the linear entropy of entanglement of the bipartition $AC|BD$, and can be expressed in terms of U^R as

$$E(U) = 1 - \frac{1}{d^4} \text{Tr}\{(U^R U^{R\dagger})^2\}. \quad (16)$$

Similarly, the operator entanglement $E(US)$ is the linear entropy of the bipartition $AD|BC$ and is

$$E(US) = 1 - \frac{1}{d^4} \text{Tr}(U^\Gamma U^{\Gamma\dagger})^2. \quad (17)$$

Whenever the subscripts on R and Γ have been dropped they can refer equally to either of the two operations. Note that the singular values of U^R and U^Γ are all local unitary invariants (LUI).

We recall definitions of some special families of unitary operators and also introduce some new families of unitary operators.

Definition 1 (Dual unitary [17]) If the realigned matrix U^R of unitary operator U is also unitary, then U is called a dual unitary.

Definition 2 (T-dual unitary [50]) If the partial transposed matrix U^Γ of a unitary operator U is also unitary, then U is called a T-dual unitary.

Definition 3 (2-unitary [48]) A unitary U for which both U^R and U^Γ are also unitary is called 2-unitary.

Definition 4 (Self dual unitary) Unitary operator U for which $U^R = U$ is called a self-dual unitary.

Note that for a 2-unitary $E(U) = E(US) = E(S) = 1 - 1/d^2$ are maximized and thus from Eq. (7) $e_p(U) = 1$, the maximum possible value. Thus the corresponding four-party state given by Eq. (14) is maximally entangled along all three bipartitions and is an absolutely maximally entangled state of four qudits; AME(4, d).

In the mathematics literature, the class of unitary operators which remain unitary under ‘block-transpose’ have been studied since 1989 [62–68]. Referred to as biunitaries, they are dual unitary upto multiplication by **SWAP**, and is the result of the Γ_1 operation above. However, the term “biunitary” seems to be used interchangeably for both dual and T-dual unitary operators and subsequently no special studies of 2-unitaries, that are both dual and T-dual seems to exist.

T-dual and dual unitary have very different entanglement properties, as reflected in their two most prominent representatives: the identity and the **SWAP** gate. However, they are related in the sense that every T-dual unitary U has a dual partner US (or SU). Note that if U is 2-unitary, so also are U^R and U^Γ . For example, the realignment of U^R is U itself, while $(U^R)^\Gamma = U^\Gamma S$, which is evidently unitary given that U is 2-unitary.

III. DUAL-UNITARY AND 2-UNITARY OPERATORS FROM NONLINEAR ITERATIVE MAPS

Complete parametrization of dual unitary operators for arbitrary local Hilbert space dimension d is not known in general except in the two-qubit case [17]. Several (incomplete) analytic constructions of families of dual unitary operators have been proposed based on complex Hadamard matrices [69], diagonal [53], and block-diagonal unitary matrices [50]. Here we briefly review the non-linear maps introduced in [47] to generate unitary operators which are arbitrarily close to dual unitaries.

A. Dynamical map for dual unitaries

The following map is defined on the space of bipartite unitary operators,

$$\mathcal{M}_R : \mathcal{U}(d^2) \longrightarrow \mathcal{U}(d^2).$$

One complete action of \mathcal{M}_R on a seed unitary U_0 consists of the following two steps:

- (i) *Linear part:* Realignment of U_0 : $U_0 \xrightarrow{R} U_0^R$,
- (ii) *Non-linear part:* Projection of U_0^R to the nearest unitary matrix U_1 given by its polar decomposition (PD) [70, 71]; $U_0^R = U_1 \sqrt{U_0^{R\dagger} U_0^R}$.

Note that U_0^R must be of full rank for the map to be well defined as the polar decomposition of rank deficient matrices is not uniquely defined. We write one complete action of the map on U_0 as

$$\mathcal{M}_R[U_0] := U_1.$$

After n iterations,

$$\underbrace{\mathcal{M}_R \circ \mathcal{M}_R \circ \cdots \circ \mathcal{M}_R}_{n \text{ times}}[U_0] := \mathcal{M}_R^n[U_0] = U_n.$$

For arbitrary seeds the map has been observed to converge to dual-unitaries almost certainly [47], and this is made plausible by the following observations on the fixed points of the map \mathcal{M}_R .

An important property of the map is that it *preserves the local orbit* of seed unitary U_0 in the following sense.

Proposition 1

$$\text{If } U'_0 \xrightarrow{LU} U_0, \text{ then } U'_1 = \mathcal{M}_R[U'_0] \xrightarrow{LU} U_1 = \mathcal{M}_R[U_0]. \quad (18)$$

Proof. This follows as:

$$\begin{aligned} U'_0^R &= [(u_1 \otimes u_2)U_0(v_1 \otimes v_2)]^R \\ &= (u_1 \otimes v_1^T)U_0^R(u_2^T \otimes v_2). \end{aligned} \quad (19)$$

Using the polar decomposition of U_0^R we get

$$\begin{aligned} U'_0^R &= (u_1 \otimes v_1^T)U_1\sqrt{U_0^{R\dagger}U_0^R}(u_2^T \otimes v_2) \\ &= (u_1 \otimes v_1^T)U_1(u_2^T \otimes v_2)\sqrt{U_0'^{R\dagger}U_0'^R} \\ &\equiv U'_1\sqrt{U_0'^{R\dagger}U_0'^R}. \end{aligned} \quad (20)$$

Explicitly

$$\mathcal{M}_R[U'_0] = (u_1 \otimes v_1^T)\mathcal{M}_R[U_0](u_2^T \otimes v_2). \quad (21)$$

Thus the changes in the operator entanglement under the \mathcal{M}_R map are unaffected by local unitary operations.

Analogous to the \mathcal{M}_R map for dual unitaries, one can define \mathcal{M}_Γ map to generate T-dual unitary operators. Action of \mathcal{M}_Γ on U_0 is defined as $\mathcal{M}_\Gamma[U_0] := U_1$, where U_1 is closest unitary to U_0^Γ given by its polar decomposition. Such an algorithm was independently studied in [72] to generate a special class of random structured bipartite unitary operators.

1. Dual unitaries as fixed points

Action of the map on a dual unitary U is

$$\mathcal{M}_R[U] = U^R,$$

as U^R is also unitary. Realignment operation is an involution; $(X^R)^R = X$. Hence, $\mathcal{M}_R[U^R] = U$, and

$$\mathcal{M}_R^2[U] = U, \quad (22)$$

i.e., dual unitaries are period-2 fixed points of the map. Note that self-dual unitaries ($U^R = U$) are fixed points of the \mathcal{M}_R map itself.

For two-qubit case ($d^2 = 4$) dual-unitaries appear to be the *only* fixed points of the \mathcal{M}_R^2 map. In the next section, it is shown that this is the case for different families of two-qubit seed unitaries.

However, for the two-qutrit case ($d^2 = 9$) we observed numerically that there are fixed points of the \mathcal{M}_R^2 map other than dual unitaries. In this case $U_1^R = U_0\sqrt{U_1^{R\dagger}U_1^R}$, and the pair U_0 and U_1 conspire such that they are the nearest unitary to the other's realignment. Generic seeds are neither of this kind, not do they seem to end up in such pairs. Under the map a non-dual fixed point is mapped to a unitary with same Schmidt coefficients. This suggests that these may be locally equivalent and the map may have first order fixed points other than self-dual unitaries also in $d > 2$.

For $d^2 > 9$ we have not been able to find such non-dual fixed points. The reason that the map does not converge to such fixed points is because of large dimensionality a random sampling of seed unitaries over the corresponding unitary group $\mathcal{U}(d^2)$ with $(d^2 - 1)$ number of parameters is unable to find appropriate seed unitaries which lead to such fixed points. One might also expect higher order fixed points of the map which makes the map a novel dynamical system in its own right but for the purposes of this work we will not focus on such directions.

B. Dynamical map for 2-unitaries

The set of 2-unitary operators is a common intersection of dual and T-dual unitaries. In order to generate 2-unitary operators a slightly modified map $\mathcal{M}_{\Gamma R}$ is used by incorporating also the partial transpose operation. Schematically the action of the map on seed unitary U_0 is

$$\mathcal{M}_{\Gamma R} : U_0 \xrightarrow{R} U_0^R \xrightarrow{\Gamma} (U_0^R)^\Gamma := U_0^{\Gamma R} \xrightarrow{\text{PD}} U_1. \quad (23)$$

It has been pointed out previously that sampling U_0 from the Circular Unitary Ensemble (CUE), for small local dimensions ($d^2 = 9, 16$), $U_n = \mathcal{M}_{\Gamma R}^n[U_0]$ is arbitrarily close to being 2-unitary, with a very high probability [47]. To generate 2-unitary operators in larger dimensions, one may need to start with an appropriate initial seed unitary, not just sampled from the CUE. This was done in [55] to generate a 2-unitary of order

36, which settled the long-standing problem of the existence of absolutely maximally entangled states of 4 parties in local dimensions six.

1. 2-unitaries as fixed points

An action of the $\mathcal{M}_{\Gamma R}$ map on a 2-unitary U is given by

$$\mathcal{M}_{\Gamma R}[U] = U^{\Gamma R},$$

as $U^{\Gamma R} := (U^R)^\Gamma = U^\Gamma S$ is also unitary. The combined rearrangement ΓR is not an involution like R or Γ , but is equivalent to the identity operation when composed thrice. Note that ΓR operation on the set of 4 symbols which label indices of the product basis states is $\{1, 2, 3, 4\} \xrightarrow{R} \{1, 3, 2, 4\} \xrightarrow{\Gamma} \{1, 4, 2, 3\}$. Thus, iterating ΓR thrice results in

$$\{1, 2, 3, 4\} \xrightarrow{\Gamma R} \{1, 4, 2, 3\} \xrightarrow{\Gamma R} \{1, 3, 4, 2\} \xrightarrow{\Gamma R} \{1, 2, 3, 4\}.$$

Therefore, 2-unitaries are period-3 fixed points of the $\mathcal{M}_{\Gamma R}$ map:

$$\mathcal{M}_{\Gamma R}^3[U] = U. \quad (24)$$

C. Structured dual unitaries from stochastic maps

Analytic constructions of dual unitaries are obtained by multiplying T-dual unitaries with the swap S . The families of T-dual unitary operators that have been analytically constructed so far, mostly have a block-diagonal structure, or are permutations (which can also be block-diagonal) [50, 73]. Dual-unitary permutations preserve dual-unitarity under multiplication (both left as well as right) by arbitrary diagonal unitaries [50]. We refer to this property of dual unitary permutations as an emphasing symmetry, and is a kind of gauge freedom enjoyed by these matrices. This symmetry is also present in the uniform block-diagonal constructions. The iterative algorithms discussed above, in general, do not lead to dual unitaries with this symmetry. In these cases, no special structure of dual is usually evident, as illustrated in Fig. (1).

In this section we demonstrate that modified algorithms can be defined that are capable of resulting in dual and 2-unitaries with block-diagonal structures or emphased permutations, and hence afford some degree of control or design. This is achieved by incorporating in the algorithm random diagonal unitaries which preserve the dual-unitary property of structured matrices.

One such algorithm \mathbb{M}_R which converges to dual unitaries with the emphasing symmetry is defined as

$$\mathbb{M}_R : U_0 \xrightarrow{R} U_0^R \xrightarrow{\text{PD}} U'_1 \rightarrow U_1 = D_1 U'_1 D_2, \quad (25)$$

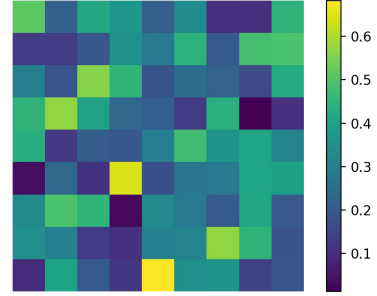


FIG. 1. Action of \mathcal{M}_R map, 1000 times, on a random seed unitary of size $d^2 = 9$ results in an approximate dual unitary which have typically all d^4 entries non-zero. Shown are the absolute value of the matrix elements in one such instance.

where D_1, D_2 are diagonal unitaries with random phases. Note that the map is no longer deterministic, as U_0 does not uniquely determine U_1 . The map converges (in all cases that we have encountered for $d = 2, 3, 4$) to dual unitaries that remain dual-unitary on multiplication by arbitrary diagonal unitaries.

Starting from a random seed unitary U_0 , the map converges to dual unitaries with different block structures as shown in Fig. (2) for $d^2 = 9$. For the sake of convenience we have shown the non-zero elements of the corresponding T-dual unitary to the dual-unitary obtained from the map. It is known that a block-diagonal unitary of size d^2 is T-dual if the size of each block is a multiple of d [50]. The map indeed yields T-dual unitaries which are block-diagonal and size of each block is multiple of d as shown in Fig. (2) for $d^2 = 9$. The resulting dual unitaries are of the following form (up to multiplication by S):

$$(i) U = \bigoplus_{i=1}^3 u_i, u_i \in \mathcal{U}(3).$$

$$(ii) U = u_1 \oplus u_2, u_1 \in \mathcal{U}(6), u_2 \in \mathcal{U}(3).$$

Due to their peculiar structure these dual unitaries remain dual-unitary under multiplication by random diagonal unitaries. This is easy to see for the uniform block case as compared to the non-uniform case in Fig. (2). In the nonuniform case, the 6×6 block cannot be replaced by an arbitrary unitary matrix. In fact 6×6 unitary matrix acting on $\mathcal{C}^2 \otimes \mathcal{C}^3$ should satisfy T-dual unitarity [50]. If we require in addition that the duality (or T-duality equivalently) is preserved under multiplication by diagonal unitaries, a subset is picked, an example being shown in Fig. (2). Note the peculiar structure of the 6×6 block in the non-uniform case. It consists of three 2×2 unitary matrices arranged in such a way that multiplication by arbitrary diagonal unitaries preserves T-duality.

We have checked that similar structured matrices are obtained for $d = 4$ and 5. For $d^2 = 16$, the map yields

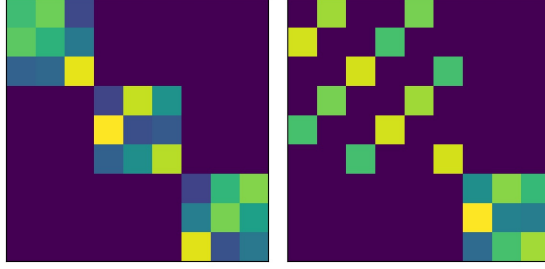


FIG. 2. (Color online) Structured T-dual unitaries obtained using the \mathcal{M}_R map for $d = 3$. (Left) T-dual unitary consisting of three blocks (unitary matrices) of size 3. (Right) T-dual unitary with a 6×6 block and a 3×3 block.

dual unitaries which are of the following forms (up to multiplication by S),

- (i) $U = \bigoplus_{i=1}^4 u_i$, $u_i \in \mathcal{U}(4)$,
- (ii) $U = \bigoplus_{i=1}^2 u_i$, $u_i \in \mathcal{U}(8)$, and
- (iii) $U = \bigoplus_{i=1}^2 u_i$, $u_1 \in \mathcal{U}(4)$, $u_2 \in \mathcal{U}(12)$.

These block structures are compatible with the analytical constructions of dual unitary operators based on block-diagonal unitaries.

To obtain structured 2-unitaries, we define $\mathcal{M}_{\Gamma R}$ map as follows,

$$U_0 \xrightarrow{R} U_0^R \xrightarrow{\Gamma} \left(U_0^R \right)^\Gamma := U_0^{\Gamma R} \xrightarrow{\text{PD}} U_1' \rightarrow U_1 = D_1 U_1' D_2. \quad (26)$$

For $d^2 = 9$, it is observed that for a random seed unitary if the map converges to 2-unitary then it is a 2-unitary permutation matrix up to multiplication by diagonal unitaries as shown in Fig. (3). There is only one non-zero element in each row positioned in such a way that the whole arrangement of non-zero entries in a 2-unitary permutation matrix is directly related to orthogonal Latin squares which we elaborate in next sections. The map is not as efficient as its deterministic counterpart $\mathcal{M}_{\Gamma R}$ in yielding 2-unitaries from random seed unitaries. However it demonstrates that one can obtain structured 2-unitary operators of desired symmetry and can be used to gain insights about the most general constructions of such special unitary operators. We have observed that multiplying at each step of the map with random, but structured, unitaries other than diagonal unitaries can also yield structured dual matrices, provided duality is preserved under such operations.

IV. DYNAMICAL MAP IN THE TWO-QUBIT CASE

The \mathcal{M}_R map is now studied explicitly and analytically in the case of two qubit unitary operators. The

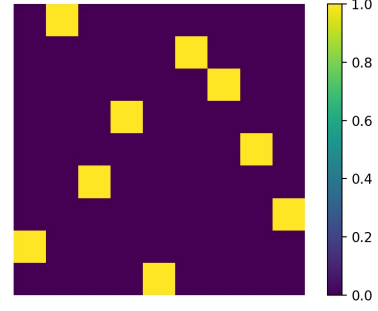


FIG. 3. Action of $\mathcal{M}_{\Gamma R}$ map on a random seed unitary of order 9. The map converges to 2-unitary permutation matrix (up to phases). The only non-zero element in each row or column is shown by a yellow square.

nonlocal part of the operators is well-known in this case. As the map has been shown to be covariant under local unitary transformations, see Eq. (18), it is sufficient to consider its action on the nonlocal part. The subset of dual-unitary matrices is known explicitly in this case and we can calculate the rate at which arbitrary seeds approach the dual set. We will find that those that approach the SWAP gate S do so algebraically slowly, while generically the approach is exponential.

Any unitary operator in $\mathcal{U}(4)$ can be written as $(u_1 \otimes u_2)U(v_1 \otimes v_2)$, where u_i and v_i are single qubit unitaries in $\mathcal{U}(2)$. In other words it is local unitarily equivalent to its nonlocal canonical Cartan form [74–76]

$$U = \exp \left[-i \sum_{k=1}^3 c_k (\sigma_k \otimes \sigma_k) \right], \quad (27)$$

where σ_k are Pauli matrices and $c_k \in \mathbb{R}$ are called *Cartan coefficients*. The so-called “Weyl chamber” [76] is a tetrahedron formed by considering the subset of c_k ’s,

$$0 \leq c_3 \leq c_2 \leq c_1 \leq \frac{\pi}{4} \quad (28)$$

The c_k ’s in the Weyl chamber which uniquely identify local unitarily inequivalent gates, is also termed as the gate’s information content [77]. For two qubit dual unitaries [17],

$$c_1 = c_2 = \frac{\pi}{4}, \quad c_3 \in \left[0, \frac{\pi}{4} \right], \quad (29)$$

and provides the complete parametrization of the non-local part. An equivalent parametrization is not known in higher dimensions.

A. \mathcal{M}_R map in the Weyl chamber

While the map has been defined on general unitary matrices, the overall phase has no impact on entanglement and the map can be defined as an action on

$SU(4)$, with $\det(U) = 1$, to itself by removing the phase at each step. This turns out to be very useful for the qubit case.

Consider a seed unitary in Cartan form as

$$U_0 = \exp \left[-i \sum_{k=1}^3 c_k^{(0)} (\sigma_k \otimes \sigma_k) \right] = \begin{pmatrix} e^{-ic_3^{(0)}} c_-^{(0)} & 0 & 0 & -ie^{-ic_3^{(0)}} s_-^{(0)} \\ 0 & e^{ic_3^{(0)}} c_+^{(0)} & -ie^{ic_3^{(0)}} s_+^{(0)} & 0 \\ 0 & -ie^{ic_3^{(0)}} s_+^{(0)} & e^{ic_3^{(0)}} c_+^{(0)} & 0 \\ -ie^{-ic_3^{(0)}} s_-^{(0)} & 0 & 0 & e^{-ic_3^{(0)}} c_-^{(0)} \end{pmatrix} \quad (30)$$

where,

$$\begin{aligned} c_{\pm}^{(n)} &= \cos(c_1^{(n)} \pm c_2^{(n)}), \\ s_{\pm}^{(n)} &= \sin(c_1^{(n)} \pm c_2^{(n)}), \quad n = 0, 1, \dots \end{aligned} \quad (31)$$

Note that $U_0 \in SU(4)$ and we would like the subsequent iterations to also satisfy this property: it also becomes easy to identify the Cartan coefficients c_i at every step. A crucial property of the map is that it preserves the matrix form of U_0 such that U_1 has exactly the same structure; see appendix (A).

Let

$$U_n = \begin{pmatrix} \alpha_n & 0 & 0 & \beta_n \\ 0 & \delta_n & \gamma_n & 0 \\ 0 & \gamma_n & \delta_n & 0 \\ \beta_n & 0 & 0 & \alpha_n \end{pmatrix} \in SU(4), \quad (32)$$

where

$$\begin{aligned} \alpha_n &= e^{-ic_3^{(n)}} c_-^{(n)}, \quad \beta_n = -ie^{-ic_3^{(n)}} s_-^{(n)}, \\ \gamma_n &= -ie^{ic_3^{(n)}} s_+^{(n)}, \quad \delta_n = e^{ic_3^{(n)}} c_+^{(n)}, \end{aligned} \quad (33)$$

The mapping between matrix elements of U_{n+1} and U_n is given by

$$\begin{aligned} \alpha_{n+1} &= \frac{e^{-i\frac{\chi_{n+1}}{4}}}{2} \left[\frac{\alpha_n + \delta_n}{|\alpha_n + \delta_n|} + \frac{\alpha_n - \delta_n}{|\alpha_n - \delta_n|} \right] \\ \beta_{n+1} &= \frac{e^{-i\frac{\chi_{n+1}}{4}}}{2} \left[\frac{\alpha_n + \delta_n}{|\alpha_n + \delta_n|} - \frac{\alpha_n - \delta_n}{|\alpha_n - \delta_n|} \right] \\ \gamma_{n+1} &= \frac{e^{-i\frac{\chi_{n+1}}{4}}}{2} \left[\frac{\beta_n + \gamma_n}{|\beta_n + \gamma_n|} - \frac{\beta_n - \gamma_n}{|\beta_n - \gamma_n|} \right] \\ \delta_{n+1} &= \frac{e^{-i\frac{\chi_{n+1}}{4}}}{2} \left[\frac{\beta_n + \gamma_n}{|\beta_n + \gamma_n|} + \frac{\beta_n - \gamma_n}{|\beta_n - \gamma_n|} \right], \end{aligned} \quad (34)$$

where

$$\chi_{n+1} = \text{Arg}[(\alpha_n^2 - \delta_n^2)(\beta_n^2 - \gamma_n^2)]. \quad (35)$$

The dynamical system is thus a 4-dimensional complex map on the manifold $S^4 \times S^4$. There are constraints originating from the unitarity condition: $|\alpha_i|^2 + |\beta_i|^2 = 1$, $|\gamma_i|^2 + |\delta_i|^2 = 1$, $\text{Re}(\alpha_i \beta_i^*) = 0$ and $\text{Re}(\gamma_i \delta_i^*) = 0$, and the SU condition: $(\alpha_n^2 - \beta_n^2)(\delta_n^2 - \gamma_n^2) = 1$. The non-linear nature of the map is clear as the entries of the above transformation are themselves functions of other variables.

Rather than the high-dimensional complex map in Eq. (34), using Eq. (33) one obtains a 3-dimensional real map in terms of the Cartan coefficients. Defining $\theta_{\pm}^{(n)} = \text{Arg}(\alpha_n \pm \delta_n)$ and $\phi_{\pm}^{(n)} = \text{Arg}(\beta_n \pm \gamma_n)$, the complex map in Eq. (34) simplifies to

$$\begin{aligned} c_1^{(n+1)} &= \frac{1}{4}(-\theta_+^{(n)} + \theta_-^{(n)} - \phi_+^{(n)} + \phi_-^{(n)}), \\ c_2^{(n+1)} &= \frac{1}{4}(\theta_+^{(n)} - \theta_-^{(n)} - \phi_+^{(n)} + \phi_-^{(n)}), \\ c_3^{(n+1)} &= \frac{1}{4}(-\theta_+^{(n)} - \theta_-^{(n)} + \phi_+^{(n)} + \phi_-^{(n)}). \end{aligned} \quad (36)$$

Numerically it is observed that the Cartan coefficients of $U_{n+1} = \mathcal{M}_R[U_n]$ obtained from the above 3-dimensional map agree for all even n with those calculated using the numerical algorithm presented in Ref. [77] and also satisfy Eq. (28). However for odd n although $c_3^{(n)}$ values still agree but $c_1^{(n+1)}$ and $c_2^{(n+1)}$ values differ from the numerical value by $\pi/2$. In order to obtain the desired Cartan coefficients satisfying Eq. (28) from the above 3-dimensional map, one needs to replace $c_2^{(n+1)}$ by $\pi/2 - c_2^{(n+1)}$ for all odd n .

Before we simplify the 3-dimensional map given by Eq. (36), we first prove the following theorem.

Theorem 1 For two-qubit gates of the form Eq. (27) self-dual unitaries ($U = U^R$) are the only fixed points of the \mathcal{M}_R map.

Proof. Let U_0 be a two-qubit gate of the form in Eq. (32). If U_0 is fixed point of the \mathcal{M}_R map:

$$\mathcal{M}_R[U_0] = U_1 = U_0. \quad (37)$$

As this implies that U_1 is also in $SU(4)$, $\chi_1 = 0$. Using Eq. (34), in particular $\alpha_1 = \alpha_0$ implies that

$$\begin{aligned} \text{Re } \alpha_1 &= \frac{1}{2} \left[\frac{c_-^{(0)} + c_+^{(0)}}{|\alpha_0 + \delta_0|} + \frac{c_-^{(0)} - c_+^{(0)}}{|\alpha_0 - \delta_0|} \right] \cos c_3^{(0)} \\ &= \text{Re } \alpha_0 = \cos c_3^{(0)} c_-^{(0)}. \end{aligned} \quad (38)$$

The range of the parameters in the Weyl chamber, Eq. (28) implies that $\cos c_3^{(0)} \neq 0$. Similarly,

$$\begin{aligned} \text{Im } \alpha_1 &= \frac{1}{2} \left[\frac{-c_-^{(0)} + c_+^{(0)}}{|\alpha_0 + \delta_0|} - \frac{c_-^{(0)} + c_+^{(0)}}{|\alpha_0 - \delta_0|} \right] \sin c_3^{(0)} \\ &= \text{Im } \alpha_0 = -\sin c_3^{(0)} c_-^{(0)}. \end{aligned} \quad (39)$$

The case of $c_3^{(0)} = 0$ is dealt with separately below where we explicitly show that U_1 is self-dual. Assuming that $c_3^{(0)} \neq 0$, the above set of equations imply that $c_+^{(0)} = \cos(c_1^{(0)} + c_2^{(0)}) = 0$. Given the range of these parameters, this fixes uniquely $c_1^{(0)} = c_2^{(0)} = \pi/4$, which implies from Eq. (33) that $\beta_0 = \delta_0 = 0$. Therefore $\mathcal{M}_R[U_0] = U_0$ implies

$$U_0 = \begin{pmatrix} \alpha_0 & 0 & 0 & 0 \\ 0 & 0 & \gamma_0 & 0 \\ 0 & \gamma_0 & 0 & 0 \\ 0 & 0 & 0 & \alpha_0 \end{pmatrix}, \quad (40)$$

and hence U_0 is a self-dual unitary, *i.e.* $U_0^R = U_0$.

Consider a two-qubit seed unitary U_0 parametrized by the Cartan parameters $c_1^{(0)}, c_2^{(0)}, c_3^{(0)}$. Under the \mathcal{M}_R map U_0 is mapped to U_1 which is parametrized by $c_1^{(1)}, c_2^{(1)}, c_3^{(1)}$. The \mathcal{M}_R map can be viewed most economically as a 3-dimensional dynamical map on the Cartan parameters,

$$\begin{aligned} U_n &\xrightarrow{\mathcal{M}_R} U_{n+1}, \\ (c_1^{(n)}, c_2^{(n)}, c_3^{(n)}) &\xrightarrow{\mathcal{M}_R} (c_1^{(n+1)}, c_2^{(n+1)}, c_3^{(n+1)}). \end{aligned} \quad (41)$$

B. Deriving the map for special initial conditions

Although we are unable to derive explicit maps in terms of these parameters for general $c_i^{(0)}$, we are able to do so for special values. We show that these converge to the desired fixed points, $c_1^{(n \rightarrow \infty)} = \frac{\pi}{4}$, $c_2^{(n \rightarrow \infty)} = \frac{\pi}{4}$, and $c_3^{(n \rightarrow \infty)} \in [0, \frac{\pi}{4}]$, which is the set of dual-unitary operators. This is depicted in Fig. (4) for few random realizations evolved under the map for $n = 10$ steps. For the general case we argue why this happens and also derive the rate of exponential approach.

1. XY family: plane $c_3 = 0$

The first special case is when $c_3^{(0)} = 0$ and $0 < c_2^{(0)} \leq c_1^{(0)}$. In this case, using Eq. (34), we can see that a *single* application of the \mathcal{M}_R map results in the following unitary:

$$U_1 = \begin{pmatrix} 1 & 0 & 0 & 0 \\ 0 & 0 & -i & 0 \\ 0 & -i & 0 & 0 \\ 0 & 0 & 0 & 1 \end{pmatrix},$$

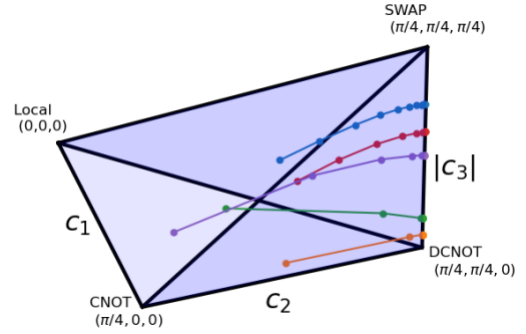


FIG. 4. Trajectories of five random realizations of two-qubit gates are shown inside the Weyl chamber under action of the map for $n = 10$ steps. The edge joining the SWAP gate and the DCNOT gate corresponds to dual unitaries to which the map converges.

with $\det(U_1) = \det(U_0) = 1$. Thus the map preserves the SU property of seed unitaries. Cartan parameters for U_1 are: $c_1^{(1)} = c_2^{(1)} = \pi/4$, $c_3^{(1)} = 0$, and therefore U_1 is dual-unitary. This gate is LU equivalent to the gate DCNOT [77] which is $S \times \text{CNOT}$. Explicitly,

$$\begin{aligned} U_{\text{DCNOT}} &= (H \otimes I) U_1 (D_1 \otimes D_1 H) \\ &= \begin{pmatrix} 1 & 0 & 0 & 0 \\ 0 & 0 & 0 & 1 \\ 0 & 1 & 0 & 0 \\ 0 & 0 & 1 & 0 \end{pmatrix}, \end{aligned} \quad (42)$$

where $H = \frac{1}{\sqrt{2}} \begin{pmatrix} 1 & 1 \\ 1 & -1 \end{pmatrix}$ is the Hadamard gate and $D_1 = P_{\frac{\pi}{2}} = \begin{pmatrix} 1 & 0 \\ 0 & i \end{pmatrix}$ is a phase gate.

Thus the entire interior of the base of the Weyl chamber, $c_3 = 0$ plane, is mapped to the same dual-unitary gate U_1 in just one step and the rate at which it happens is infinite.

2. XXX family: $c_1 = c_2 = c_3$

Let $c_1 = c_2 = c_3 = c \in [0, \pi/4]$ in Eq. (27), the single parameter family of unitary operators U ,

$$U = \exp \left(-i c \sum_{i=1}^3 \sigma_i \otimes \sigma_i \right). \quad (43)$$

This forms an edge of the Weyl chamber, the one that connects local unitaries to the SWAP gate S . Unitaries of this form are useful in many contexts such as in the trotterization of integrable isotropic (XXX) Heisenberg Hamiltonian [78]. They are also, modulo

phases, the fractional powers of the **SWAP** gate S as $U = \exp(-2icS)$.

If we choose the seed unitary U_0 from this family with $c = c^{(0)}$, it follows from Eq. (33) that $\beta_0 = 0$. Action of the map on U_0 gives

$$U_1 = \begin{pmatrix} \alpha_1 & 0 & 0 & \beta_1 \\ 0 & 0 & \gamma_1 & 0 \\ 0 & \gamma_1 & 0 & 0 \\ \beta_1 & 0 & 0 & \alpha_1 \end{pmatrix}, \quad (44)$$

for which $\delta_1 = 0$. Note that U_1 is not exactly of the same form as U_0 for which $\beta_0 = 0$. In fact for all even (odd) n , U_n is such that $\beta_n = 0$ ($\delta_n = 0$). For even n , $\beta_n = 0$ implies $c_1(n) = c_2(n)$ both being equal to $c_3^{(n)}$ and thus U_n belongs to the same family. However, for odd n it is observed that although $c_2^{(n)} = c_3^{(n)} \leq \pi/4$, $c_1^{(1)} = \pi/2 - c_2^{(1)} \geq \pi/4$ and thus $c_1^{(1)}$ does not satisfy Eq. (28). Note that U_1 with Cartan coefficients $c_1^{(1)} = \pi/2 - c^{(1)}$, $c_2^{(n)} = c_3^{(1)} = c^{(1)}$ is *not* LU equivalent to a gate with Cartan coefficients $c_1^{(n)} = c_2^{(n)} = c_3^{(1)} = c^{(1)}$, although in the part of the Weyl chamber we are restricted attention to, they are the same points.

As a consequence of this, the 3-dimensional map given by Eq. (36) becomes a 1-dimensional map.

Let $c^{(n)}$ be the Cartan coefficient parametrizing $U_n = \mathcal{M}_R^n[U_0]$, and

$$x_n = 1/\tan(2c^{(n)}). \quad (45)$$

The complications attendant on the ranges of c_i do not affect this variable. In terms of x_n (for a derivation see App. (B)), the map takes a simple algebraic form,

$$x_{n+1} = \frac{2x_n}{1 + \sqrt{4x_n^2 + 1}}. \quad (46)$$

The unique fixed point of the map is $x^* = 0$ corresponding to the **SWAP** gate, and the map is a contraction as shown in the App. (B). Therefore, in the limit of large n , $x_n \rightarrow x^* = 0$. In this limit, Eq. (46) can be approximated as

$$x_{n+1} \approx x_n(1 - x_n^2). \quad (47)$$

Thus in the vicinity of the fixed point, the difference equation may be approximated by the differential equation $dx_n/dn = -x_n^3$. This is simple to solve and gives the large n approximation to the map above as

$$x_n \approx 1/\sqrt{2n}. \quad (48)$$

3. SWAP-CNOT-DCNOT face; $c_1^{(0)} = \pi/4$

In this case seed unitaries lie on the SWAP-CNOT-DCNOT face of the Weyl chamber with $c_1^{(0)} = \pi/4$. Under the action of the map $c_1^{(n)} = \pi/4$ for all n and thus the corresponding map is 2-dimesional defined in terms of $c_2^{(n)}$ and $c_3^{(n)}$. An important property of the map observed in this case, which follows as $c_{\pm} = s_{\mp}$, is that the phase in Eq. (34) $\chi_{n+1} = 0$. This property is crucial for simplifying the map as shown below.

Defining $y_n = 1/\tan^2(2c_2^{(n)})$ and $z_n = 1/\tan^2(2c_3^{(n)})$, the corresponding 2-dimensional map takes a purely algebraic form given by (for a derivation see App. (B))

$$\begin{aligned} y_{n+1} &= \frac{y_n}{1 + z_n}, \\ z_{n+1} &= \frac{z_n}{1 + y_n}. \end{aligned} \quad (49)$$

Although the above map has a symmetric form, due to the specific choice of Cartan parameters Eq. (28), the symmetry is broken and the fixed points are $y^* = 0$ (or $c_2^{(\infty)} = \pi/4$) and $z^* \in [0, \infty]$ (or $c_3^{(\infty)} \in [0, \pi/4]$) corresponding to the set of dual unitaries. This 2-dimensional map can be solved analytically by noting that

$$\Omega = \frac{1 + y_{n+1}}{1 + z_{n+1}} = \frac{1 + y_n}{1 + z_n} \quad (50)$$

is an invariant. Its value is determined by the initial conditions as:

$$\Omega = \frac{1 + y_0}{1 + z_0} = \left(\frac{\sin(2c_3^{(0)})}{\sin(2c_2^{(0)})} \right)^2 < 1 \quad (51)$$

for $c_3^{(0)} < c_2^{(0)}$.

Using this to eliminate z_n , we have the 1-dimensional map:

$$y_{n+1} = \Omega \frac{y_n}{1 + y_n}, \quad (52)$$

which has the exact solution

$$y_n = \frac{\Omega^n y_0}{1 + \left(\frac{1 - \Omega^n}{1 - \Omega} \right) y_0}, \quad (53)$$

and implies that

$$z_n = \frac{z_0}{\Omega^n + \left(\frac{1 - \Omega^n}{1 - \Omega} \right) \Omega z_0}. \quad (54)$$

It follows from Eq. (53) that $y_\infty = 0$ and $z_\infty = \frac{1}{\Omega} - 1$ respectively. Also $c_3^{(\infty)}$ which parametrizes the dual unitary to which the map converges can be written explicitly in terms of the initial pair $(c_2^{(0)}, c_3^{(0)})$ as

$$\begin{aligned} c_3^{(\infty)} &= \frac{1}{2} \arctan \left[\sqrt{\frac{\Omega}{1-\Omega}} \right] \\ &= \frac{1}{2} \arctan \left[\frac{\sin(2c_3^{(0)})}{\sqrt{\sin^2(2c_2^{(0)}) - \sin^2(2c_3^{(0)})}} \right]. \end{aligned} \quad (55)$$

Defining $\Delta c_i^{(n)} = c_i^{(\infty)} - c_i^{(n)}$ where $c_1^{(\infty)} = c_2^{(\infty)} = \pi/4$. Note that $\Omega = \sin^2(2c_3^{(\infty)})$, governs the exponential approach to the duals. From the explicit and full solution in Eq. (53) it follows that

$$\begin{aligned} \Delta c_2^{(n)} &\sim |\sin 2c_3^{(\infty)}|^n, \\ \Delta c_3^{(n)} &\sim |\sin 2c_3^{(\infty)}|^{2n}. \end{aligned} \quad (56)$$

We will see below that these continue to hold for the general case as well.

The marginal case $\Omega = 1$ corresponds to seed unitaries on the SWAP-CNOT edge with $c_2^{(0)} = c_3^{(0)}$ and is dealt separately below.

4. SWAP-CNOT edge

For these gates $c_1^{(0)} = \pi/4$, $c_2^{(0)} = c_3^{(0)}$ and is a special case of the face just discussed. In this case, the 2-dimensional map Eq. (49) degenerates to a 1-dimensional map given by

$$y_{n+1} = \frac{y_n}{1+y_n}, \quad (57)$$

with $\Omega = 1$. This map also can be solved analytically and the solution is given by

$$y_n = \frac{y_0}{\sqrt{n y_0^2 + 1}}. \quad (58)$$

The approach to the unique fixed point $y^* = 0$ is algebraic in contrast to other gates on the SWAP-CNOT-DCNOT face and goes as $\sim 1/\sqrt{n}$. Thus the SWAP gate is approached slowly along both the edges that connect it in the Weyl chamber from the locals or from the CNOT gates. The other edge is the dual-unitary edge that is already a line of fixed points. In fact the entire face of the Weyl chamber containing locals-SWAP-CNOT is mapped into itself and all initial conditions on this approach the dual-unitary SWAP gate algebraically. This face is characterized by two of the Cartan coefficients being equal, namely $c_2^{(n)} = c_3^{(n)} \equiv c^{(n)}$. In the limit of large n , $\Delta c_1^{(n)} = \pi/4 - c_1^{(n)} \sim 1/n$ while $\Delta c_2^{(n)} = \Delta c_3^{(n)} = \pi/4 - c^{(n)} \sim 1/\sqrt{n}$.

5. XXZ family: $c_1 = c_2$

Let us consider now a family of two-qubit gates for which $c_1^{(0)} = c_2^{(0)} = c^{(0)} \in (0, \frac{\pi}{4}]$, and $c_3^{(0)} \leq c^{(0)} \in [0, \frac{\pi}{4}]$. This restricts the seed unitaries to the face of the Weyl chamber that contains locals-SWAP-DCNOT. Under the action of the map the unitaries remain on this face for even n and up to a local unitary transformation for odd n .

The map is 2-dimensional defined on $c_1^{(n)} = c_2^{(n)} = c^{(n)} \leq \pi/4$ and $c_3^{(n)} \leq c^{(n)}$ is given by

$$c^{(n+1)} = \frac{\pi}{4} - \frac{1}{4} \arctan \left\{ \frac{1}{2} \sin(2c_3^{(n)}) \left[\frac{1}{\tan^2(c^{(n)})} - \tan^2(c^{(n)}) \right] \right\}, \quad (59)$$

$$c_3^{(n+1)} = \frac{c_3^{(n)}}{2} + \frac{1}{4} \arctan \left\{ \frac{1}{2} \tan(2c_3^{(n)}) \left[\frac{1}{\tan^2(c^{(n)})} + \tan^2(c^{(n)}) \right] \right\}, \quad (60)$$

The fixed points consist of $c^* = \pi/4$ and c_3^* can take any value in $[0, \frac{\pi}{4}]$ which is a line of fixed points corresponding to two-qubit dual unitaries. It is not hard to see that these are the only fixed points of the map.

The important information about the nature of the map can be obtained in the large n limit, which is effectively a linear stability analysis. Defining $\Delta c_i^{(n)} =$

$c_i^{(\infty)} - c_i^{(n)}$ where $c_1^{(\infty)} = c_2^{(\infty)} = \pi/4$. For small $\Delta c^{(n)}$, Eq. (59) gives

$$\Delta c^{(n+1)} \approx \sin(2c_3^{(n)}) \Delta c^{(n)}. \quad (61)$$

Whereas Eq. (60) yields simply $c_3^{(n+1)} \approx c_3^{(n)}$ to first order in X_n indicating that it can take any value only determined by the initial condition. We denote this value

as $c_3^* = c_3^{(\infty)}$. Thus the above equation is of the form, $\Delta c^{(n+1)} = r \Delta c^{(n)}$, with $r = \sin(2 c_3^{(\infty)})$, and we get the solution:

$$\Delta c^{(n)} = e^{-n\xi} \Delta c^{(0)}, \quad \xi = |\ln r| = |\ln \sin(2 c_3^{(\infty)})| \quad (62)$$

Therefore, the convergence to the respective fixed points: $c^* = \frac{\pi}{4}$ and $c_3^* = c_3^{(\infty)} \in [0, \pi/4]$, is also exponential with the rate determined by the value $c_3^{(\infty)}$ as found in Eq. (56) for gates lying on the SWAP-CNOT-DCNOT face. This is shown qualitatively in Fig. (5). The rate $\xi = \infty$ when $c_3^{(\infty)} = 0$ and the unitaries converge to the DCNOT. This is consistent with the discussion in the XY discussion above where it was shown that in this case just one step of the map is needed. The rate $\xi = 0$ when $c_3^{(\infty)} = \pi/4$ when the gate attained asymptotically is the SWAP. This is consistent with the discussion of the edge XXX above where an algebraic approach was obtained.

For large n the behaviour of $\Delta c_3^{(n+1)} = c_3^{(\infty)} - c_3^{(n)}$ is found by analyzing Eq. (60) keeping the second order terms in $\Delta c^{(n)}$, and we get

$$\Delta c_3^{(n+1)} = \frac{1}{2} \sin(4c_3^{(\infty)}) (\Delta c^{(n)})^2 = \frac{1}{2} \sin(4c_3^{(\infty)}) e^{-n\xi_3}, \quad (63)$$

with $\xi_3 = 2\xi$, and hence the approach to $c_3^{(\infty)}$ is exponential at a rate that is *twice* that of the other Cartan parameters.

6. Generic initial conditions

Interestingly, numerical results indicate that the exponential approach to $(\pi/4, \pi/4, c_3^{(\infty)})$ given in Eq. (62) and Eq. (63) continues to hold for a generic initial condition inside the Weyl chamber. An illustration is displayed in Fig. (6) for the initial condition $(c_1^{(0)}, c_2^{(0)}, c_3^{(0)}) = (\pi/6, \pi/8, \pi/12)$. Under the map it converges to a dual-unitary gate with $c_3^\infty \approx 0.443$. The rates ξ_1 and ξ_2 at which $\Delta c_1^{(n)} = \pi/4 - c_1^{(n)}$ and $\Delta c_2^{(n)} = \pi/4 - c_2^{(n)}$ approach 0 are almost the same given by $\xi = |\ln \sin(2 c_3^{(\infty)})|$. The rate ξ_3 at which $\Delta c_3^{(n)} = c_3^{(\infty)} - c_3^{(n)} \rightarrow 0$ continues to be a very good approximation $\xi_3 = 2\xi$. Initial conditions which converge to dual-unitaries with large $c_3^{(\infty)}$ values *i.e.*, small entangling power, take longer times. This is reflected in Fig. (4) for random realizations where gates that are closer to the SWAP gate take longer to reach the corresponding point on the dual-unitary edge.

We summarize the convergence of the map for different families in Table I. The slow algebraic approach

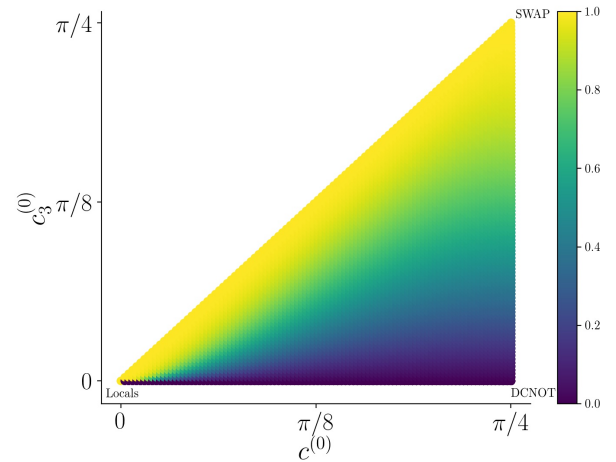


FIG. 5. Convergence in the XXZ case: initial condition in the local-SWAP-DCNOT face. Plotted is $r = \sin(2c_3^{(100)}) \approx \sin(2c_3^{(\infty)})$, which is related to the rate of convergence to a dual-unitary gate as $\xi = \ln r$. Around 10^5 initial conditions $(c_1^{(0)}, c_2^{(0)}, c_3^{(0)})$ are taken and evolved for $n = 100$ times under the 2-d map Eqs. (59)–(60). Initial conditions with $c_3^{(0)} = 0$, in the base of the triangle above, converge to the DCNOT gate at an infinite rate, while initial conditions with $c_3^{(0)} \in (0, \pi/4]$ converge to the SWAP gate at vanishing rate, namely algebraically.

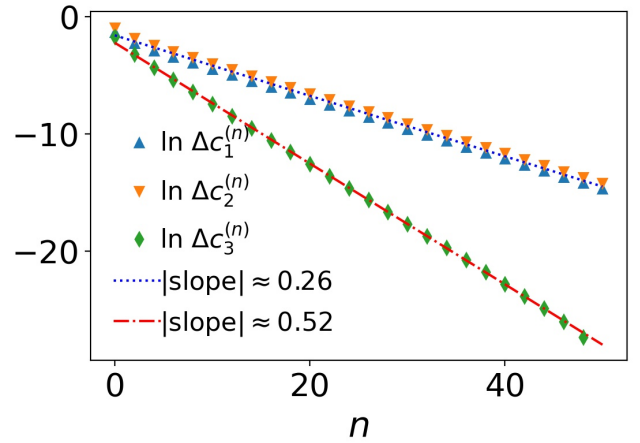


FIG. 6. Convergence for initial condition inside the Weyl chamber: seed unitary with $(c_1^{(0)}, c_2^{(0)}, c_3^{(0)}) = (\pi/6, \pi/8, \pi/12)$ is evolved under the map for $n = 50$ steps. The exponential rates at which $\Delta c_1^{(n)} = \pi/4 - c_1^{(n)}$ and $\Delta c_2^{(n)} = \pi/4 - c_2^{(n)}$ decay are almost the same $\xi = |\ln \sin(2 c_3^{(\infty)})|$ determined by $c_3^{(\infty)} \approx 0.443$. Rate at which $\Delta c_3^{(n)} = c_3^{(\infty)} - c_3^{(n)} \rightarrow 0$ is almost twice than that of $\Delta c_1^{(n)}$ or $\Delta c_2^{(n)}$. The numerically calculated slopes match with these values.

hold for all initial conditions that approach the SWAP gate. In fact, we have numerically verified that even for higher dimensions, $d > 2$, if the seed unitary is a fractional power of SWAP, they approach the dual-unitary SWAP gate algebraically as $\sim 1/\sqrt{n}$.

It maybe noted that a very different map on the Weyl chamber has been studied by looking at the the powers of two-qubit gates in Ref. [79]. This map is ergodic on the Weyl chamber and is related to billiard dynamics in a tetrahedron, unlike the dissipative nature of the \mathcal{M}_R map that we have studied.

V. COMBINATORIAL DESIGNS CORRESPONDING TO DUAL UNITARY OPERATORS

Tools developed in combinatorial mathematics have been very useful in constructing multipartite entangled states [48, 58]. In Ref. [59] it was shown that orthogonal Latin squares of order d can be used to construct 2-unitary permutation matrices of order d^2 . Since 2-unitary operators belong to a subset of dual-unitary operators, we point to less restrictive combinatorial structures corresponding to general dual-unitary operators. In the case of dual-unitary permutations such designs were discussed earlier in [80], which we first summarize.

A. Permutation matrices: classical design

A permutation of d^2 symbols or elements from $[d] \times [d]$, $[d] = \{1, 2, \dots, d\}$, is specified by the operator on computational product basis states $|ij\rangle$ as,

$$P|ij\rangle = |k_{ij}l_{ij}\rangle. \quad (64)$$

Thus, this can be written in terms of a pair of $d \times d$ matrices $K = (k_{ij})$ and $L = (l_{ij})$. In [50], it was shown that for P to be dual-unitary (T-dual), the conditions on K and L matrices are:

- (i) *Condition on K*: No element repeats along any row (column).
- (ii) *Condition on L*: No element repeats along any column (row).

As an example, for $d = 2$, the dual-unitary SWAP gate permutes the basis states as

$$\begin{bmatrix} 11 & 12 \\ 21 & 22 \end{bmatrix} \longrightarrow \begin{bmatrix} 11 & 21 \\ 12 & 22 \end{bmatrix}, \quad (65)$$

with K and L given by

$$K = \begin{bmatrix} 1 & 2 \\ 1 & 2 \end{bmatrix}, \quad L = \begin{bmatrix} 1 & 1 \\ 2 & 2 \end{bmatrix}. \quad (66)$$

Orthogonal Latin squares, denoted $OLS(d)$ [81], are examples of designs used to construct the 2-unitary operators [59]. A Latin square is a $d \times d$ array with d distinct elements such that every element appears exactly once in each column and in each row. Two Latin squares with elements s_{ij} and t_{ij} are orthogonal if the ordered pairs (s_{ij}, t_{ij}) are all distinct.

If K and L , defined above, are Latin squares, then the corresponding permutation matrix P is both dual-unitary and T-dual, hence it is 2-unitary. $OLS(d)$ exist for all d except $d = 2$ and 6 [82]. Thus 2-unitary permutations exist for all d except $d = 2$ and 6 . An example of an $OLS(3)$ is:

$$\begin{array}{|c|c|c|} \hline 1 & 2 & 3 \\ \hline 3 & 1 & 2 \\ \hline 2 & 3 & 1 \\ \hline \end{array} \cup \begin{array}{|c|c|c|} \hline 1 & 3 & 2 \\ \hline 3 & 2 & 1 \\ \hline 2 & 1 & 3 \\ \hline \end{array} = \begin{array}{|c|c|c|} \hline 11 & 23 & 32 \\ \hline 33 & 12 & 21 \\ \hline 22 & 31 & 13 \\ \hline \end{array}. \quad (67)$$

Note that all nine pairs from the set $\{1, 2, 3\} \times \{1, 2, 3\} = \{11, 12, \dots, 32, 33\}$ are present.

For dual-unitary or, T-dual permutations K and L are not Latin squares in general. We define *r-Latin square* (*c-Latin square*) as an arrangement of d symbols in a $d \times d$ array if it satisfies conditions of a Latin square only along rows (columns). Note that the usual Latin square is both r-Latin square as well as c-Latin square. Two such less constrained Latin squares are orthogonal if by superposing them all d^2 ordered pairs obtained are distinct. For dual-unitary permutations K is r-Latin square and L is c-Latin square while for T-dual permutations K is c-Latin square and L is r-Latin square, which are restatements of the conditions above for duality(T-duality).

B. General dual-unitary operators: Quantum design

Here we discuss the underlying combinatorial structure of general dual-unitary operators. Consider a unitary operator $U \in \mathcal{B}(\mathcal{H}_d \otimes \mathcal{H}_d)$. Define

$$|\psi_{ij}\rangle = U|ij\rangle \quad i, j = 1, 2, \dots, d. \quad (68)$$

The unitarity of U imply that the set of vectors $\{|ij\rangle\}$ and $\{|\psi_{ij}\rangle\}$ forms an orthonormal basis with completeness condition $\sum_{i,j=1}^d |ij\rangle\langle ij| = I$ and $\sum_{i,j=1}^d |\psi_{ij}\rangle\langle\psi_{ij}| = I$.

Consider $|\psi_{ij}\rangle$ which is of product form

$$|\psi_{ij}\rangle = |\alpha_{ij}\rangle \otimes |\beta_{ij}\rangle. \quad (69)$$

Analogous to K and L defined in the previous section for permutation operators, we arrange d^2 single qudit

TABLE I. Convergence to dual unitaries for different two-qubit seed unitaries, parametrized by the Cartan coefficients $c_i^{(0)}$. In all cases $c_1^{(\infty)} = c_2^{(\infty)} = \pi/4$, and $\Delta c_i = c_i^{(\infty)} - c_i^{(n)}$.

Cartan coefficients and Weyl chamber location of seeds	Dual-unitary approached	Nature of convergence
Base, $c_3^{(0)} = 0, c_2^{(0)} > 0$	DCNOT, $c_3^{(1)} = c_3^{(\infty)} = 0$ SWAP $c_3^{(\infty)} = \pi/4$	Instantaneous, rate ∞
SWAP-Local Edge: $c_1^{(0)} = c_2^{(0)} = c_3^{(0)}$		Algebraic: $\Delta c_i \sim 1/\sqrt{n}$
SWAP-Local-CNOT face, $c_2^{(0)} = c_3^{(0)} \neq c_1^{(0)}$		Algebraic: $\Delta c_3, \Delta c_2 \sim 1/\sqrt{n}, \Delta c_1 \sim 1/n$
SWAP-Local-DCNOT face, $c_1^{(0)} = c_2^{(0)} \neq c_3^{(0)}$		Exponential:
SWAP-CNOT-DCNOT face, $c_1^{(0)} = \pi/4, c_2^{(0)} \neq c_3^{(0)}$		$\Delta c_1, \Delta c_2 \sim \exp(-\xi n), \Delta c_3 \sim \exp(-2\xi n)$
Interior, $c_1^{(0)} > c_2^{(0)} > c_3^{(0)}$		$\xi = \ln \sin(2c_3^{(\infty)}) $

states $|\alpha_{ij}\rangle$ and $|\beta_{ij}\rangle$ as follows:

$$\mathcal{K} = \begin{vmatrix} |\alpha_{11}\rangle & |\alpha_{12}\rangle & \cdots & |\alpha_{1d}\rangle \\ |\alpha_{21}\rangle & |\alpha_{22}\rangle & \cdots & |\alpha_{2d}\rangle \\ \vdots & \vdots & \vdots & \vdots \\ |\alpha_{d1}\rangle & |\alpha_{d2}\rangle & \cdots & |\alpha_{dd}\rangle \end{vmatrix} \quad (70)$$

$$\mathcal{L} = \begin{vmatrix} |\beta_{11}\rangle & |\beta_{12}\rangle & \cdots & |\beta_{1d}\rangle \\ |\beta_{21}\rangle & |\beta_{22}\rangle & \cdots & |\beta_{2d}\rangle \\ \vdots & \vdots & \vdots & \vdots \\ |\beta_{d1}\rangle & |\beta_{d2}\rangle & \cdots & |\beta_{dd}\rangle \end{vmatrix}$$

The conditions for U to be dual-unitary in terms of \mathcal{K} and \mathcal{L} is presented below.

Theorem 2 If every row of \mathcal{K} and every column of \mathcal{L} forms an orthonormal basis in \mathcal{H}_d , then the unitary operator $U = \sum_{i,j=1}^d |\psi_{ij}\rangle\langle ij| = \sum_{i,j=1}^d |\alpha_{ij}\beta_{ij}\rangle\langle ij|$ is dual-unitary.

Proof. The orthonormality condition on the vectors in every row of \mathcal{K} and every column of \mathcal{L} imply that $\langle \alpha_{ij}|\alpha_{ij'}\rangle = \delta_{jj'}, \sum_{j=1}^d |\alpha_{ij}\rangle\langle \alpha_{ij}| = I_d, \forall i$ and $\langle \beta_{ij}|\beta_{ij'}\rangle = \delta_{ii'}, \sum_{i=1}^d |\beta_{ij}\rangle\langle \beta_{ij}| = I_d, \forall j$. Using these conditions, it follows,

$$\begin{aligned} U^R U^{R\dagger} &= \left(\sum_{i,j=1}^d |\alpha_{ij}i\rangle\langle \beta_{ij}j| \right) \left(\sum_{i',j'=1}^d |\beta_{i'j'}i'\rangle\langle \alpha_{i'j'}j'| \right), \\ &= \left(\sum_{j=1}^d |\alpha_{ij}\rangle\langle \alpha_{ij}| \right) \otimes \left(\sum_{i=1}^d |i\rangle\langle i| \right), \\ &= I_d \otimes I_d = I_{d^2}. \end{aligned}$$

It is similarly shown that $U^{R\dagger} U^R = I_{d^2}$, and hence unitary U is dual-unitary.

The conditions on \mathcal{K} , \mathcal{L} for U to be dual-unitary are generalizations of K and L corresponding to dual-unitary permutations. In K , L the notion of symbols

being *different* in row or column is replaced by it's quantum analog, the *orthogonality* of vectors (quantum states). In fact such a generalization is known for Latin square and OLS called as quantum Latin square (QLS) [83] and orthogonal quantum Latin square (OQLS) [58, 84] respectively. A quantum Latin square is a $d \times d$ array of d -dimensional vectors such that each row and each column forms an orthonormal basis in \mathcal{H}_d . Two quantum Latin squares are orthogonal if together they form an orthonormal basis in $\mathcal{H}_d \otimes \mathcal{H}_d$. If \mathcal{K} , \mathcal{L} defined above are quantum Latin squares then U is a 2-unitary operator [58].

The fact that there are no repetitions of symbols in a Latin square in any row or column translates into orthogonality of vectors in each row and column in the corresponding QLS. The “quantumness” and equivalence between quantum Latin squares was defined in Ref. [85] in terms of the number of distinct basis vectors (up to phases), known as the *cardinality*. For QLS constructed from classical Latin squares, simply by replacing the symbol k by a basis vector $|k\rangle$ in a d dimensional space, the cardinality is d and is said to be *classical*.

Quantum Latin square with cardinality more than d cannot be obtained from classical Latin square using unitary transformations of the basis vectors and is referred to as *genuinely quantum* [85]. Quantum Latin squares with cardinality equal to d^2 , the maximum possible value, for general d and their relation to quantum sudoku is discussed in Refs. [85, 86].

For dual-unitary or, T-dual unitary operators \mathcal{K} and \mathcal{L} are not quantum Latin squares in general. We define r-quantum Latin square (c-quantum Latin square) denoted by r-QLS (c-QLS) as a $d \times d$ array of d -dimensional vectors if it satisfies conditions of a quantum Latin square only along rows (columns). Note that the quantum Latin square is both r-QLS as well as c-QLS. For dual-unitary operators \mathcal{K} is r-QLS and \mathcal{L} is c-QLS while for T-dual operators \mathcal{K} is c-QLS and \mathcal{L} is r-QLS.

Two such less constrained QLS are said to be or-

thogonal if together they form an orthonormal basis in $\mathcal{H}_d \otimes \mathcal{H}_d$. In analogy with cardinality of a quantum Latin square, we define cardinality of \mathcal{K} or \mathcal{L} as the number of distinct basis vectors (up to phases) they contain. An r-QLS or c-QLS of size d is *classical* if it contains d distinct basis vectors and *genuinely quantum* if it contains more than d distinct basis vectors. For dual-unitary permutations cardinality of \mathcal{K}, \mathcal{L} is always equal to d and are thus classical. An example of a pair of genuine r-QLS and c-QLS of size 3 are respectively,

$$\mathcal{K} : \begin{array}{|c|c|c|} \hline & |1\rangle & |2\rangle & |3\rangle \\ \hline |1\rangle & |1\rangle & |2\rangle & |3\rangle \\ \hline \frac{1}{\sqrt{2}}(|1\rangle + |2\rangle) & \frac{1}{\sqrt{2}}(|1\rangle - |2\rangle) & |3\rangle \\ \hline \end{array}, \quad (71)$$

$$\mathcal{L} : \begin{array}{|c|c|c|} \hline |1\rangle & -|1\rangle & \frac{1}{\sqrt{2}}(|1\rangle + |2\rangle) \\ \hline |2\rangle & |2\rangle & |3\rangle \\ \hline |3\rangle & |3\rangle & \frac{1}{\sqrt{2}}(|1\rangle - |2\rangle) \\ \hline \end{array}. \quad (72)$$

Note that both \mathcal{K} (r-QLS) and \mathcal{L} (c-QLS) contain five distinct basis vectors (quantum states), across two different orthonormal bases, and are thus genuinely quantum. Together \mathcal{K} and \mathcal{L} form an orthonormal basis in $\mathcal{H}_3 \otimes \mathcal{H}_3$ arranged in $d \times d$ array as,

$$\begin{array}{|c|c|c|} \hline |1\rangle \otimes |1\rangle & -|2\rangle \otimes |1\rangle & |3\rangle \otimes \frac{1}{\sqrt{2}}(|1\rangle + |2\rangle) \\ \hline |1\rangle \otimes |2\rangle & |2\rangle \otimes |2\rangle & |3\rangle \otimes |3\rangle \\ \hline \frac{1}{\sqrt{2}}(|1\rangle + |2\rangle) \otimes |3\rangle & \frac{1}{\sqrt{2}}(|1\rangle - |2\rangle) \otimes |3\rangle & |3\rangle \otimes \frac{1}{\sqrt{2}}(|1\rangle - |2\rangle) \\ \hline \end{array}. \quad (73)$$

The dual-unitary gate corresponding to the above arrangement of size 9 is,

$$U_9 = \begin{pmatrix} 1 & 0 & 0 & 0 & 0 & 0 & 0 & 0 & 0 \\ 0 & 0 & 0 & 1 & 0 & 0 & 0 & 0 & 0 \\ 0 & 0 & 0 & 0 & 0 & 0 & \frac{1}{\sqrt{2}} & \frac{1}{\sqrt{2}} & 0 \\ 0 & -1 & 0 & 0 & 0 & 0 & 0 & 0 & 0 \\ 0 & 0 & 0 & 0 & 1 & 0 & 0 & 0 & 0 \\ 0 & 0 & 0 & 0 & 0 & 0 & \frac{1}{\sqrt{2}} & -\frac{1}{\sqrt{2}} & 0 \\ 0 & 0 & \frac{1}{\sqrt{2}} & 0 & 0 & 0 & 0 & 0 & \frac{1}{\sqrt{2}} \\ 0 & 0 & \frac{1}{\sqrt{2}} & 0 & 0 & 0 & 0 & -\frac{1}{\sqrt{2}} & 0 \\ 0 & 0 & 0 & 0 & 0 & 1 & 0 & 0 & 0 \end{pmatrix}, \quad (74)$$

with $(e_p(U_9), g_t(U_9)) = (3/4, 5/8)$. This dual unitary is not locally equivalent to any dual unitary permutation matrix (corresponding \mathcal{K} and \mathcal{L} contain only three distinct vectors) with the same entangling power and gate typicality. We obtained dual-unitary U_9 using the \mathcal{M}_R map (see Sec. (III A)). This is one of the nice properties of the map that it yields structured dual-unitaries by choosing appropriate seed unitaries like permutations.

For $e_p(U) < 1$, it is relatively easier to construct dual unitaries which are LU inequivalent to dual unitary permutations with the same entangling power. However for $e_p(U) = 1$ i.e., 2-unitaries this is not the case as they satisfy additional constraints which we discuss in the next section.

C. Combinatorial structures of known families of dual unitaries

1. Diagonal ensemble

Dual unitaries have one-to-one correspondence with T-dual unitary operators which are easier to construct. Simplest ensemble of T-dual unitaries one can think of is that of diagonal unitaries with arbitrary phases, denoted D_1 . A d^2 parameter subset of dual unitaries can be obtained by (pre- or post-) multiplying diagonal unitaries with the SWAP gate S [50, 53]. It is easy to see that for dual unitaries of the form $U = D_1 S$ obtained from the diagonal ensemble,

$$U(|k\rangle \otimes |l\rangle) = D_1 S(|k\rangle \otimes |l\rangle) = \exp(i\theta_{lk})(|l\rangle \otimes |k\rangle). \quad (75)$$

Thus, the corresponding \mathcal{K} and \mathcal{L} are same as that of the SWAP gate (up to phases) and hence are classical.

2. Block-diagonal ensemble

A more general d^3 parameter family of dual unitary gates, $U = D_d S$, can be obtained from block-diagonal unitaries [50, 73, 87], given by

$$D_d = \sum_{i=1}^d |i\rangle \langle i| \otimes u_i, \quad u_i \in \mathcal{U}(d). \quad (76)$$

This is a controlled unitary from first subsystem to the second. For this family of dual unitaries the combinatorial structures are given by

$$\mathcal{K} : \begin{array}{|c|c|c|c|} \hline |1\rangle & |2\rangle & \cdots & |d\rangle \\ \hline |1\rangle & |2\rangle & \cdots & |d\rangle \\ \hline \vdots & \vdots & \vdots & \vdots \\ \hline |1\rangle & |2\rangle & \cdots & |d\rangle \\ \hline \end{array}, \quad \mathcal{L} : \begin{array}{|c|c|c|c|} \hline u_1 |1\rangle & u_2 |1\rangle & \cdots & u_d |1\rangle \\ \hline u_1 |2\rangle & u_2 |2\rangle & \cdots & u_d |2\rangle \\ \hline \vdots & \vdots & \vdots & \vdots \\ \hline u_1 |d\rangle & u_2 |d\rangle & \cdots & u_d |d\rangle \\ \hline \end{array}, \quad (77)$$

where u_i 's are related to the dual unitary $U = D_d S$ by Eq. (76). Note the orthonormality along the columns in \mathcal{L} is ensured by the identical unitary transformation of each basis vector. Although \mathcal{K} contains only d distinct vectors and is classical however \mathcal{L} contains in general (the maximum possible) d^2 number of distinct vectors and hence is genuinely quantum.

The quantum designs considered so far are mostly unentangled, such as the ones above. Generalizations to entangled designs are needed to describe for example the recently found 2-unitary operator behind the AME(4,6) state [55]. Although one can write necessary and sufficient conditions for U to be 2-unitary; see Appendix (C), in terms of reduced density matrices of bipartite states defined in Eq. (68) but the orthogonality relations in the corresponding OQLS are harder to interpret than in OLS.

VI. LOCAL UNITARY EQUIVALENCE OF 2-UNITARY OPERATORS

A. A necessary criterion

Given any two bipartite unitary operators U and U' , as far as we know, there is no procedure to determine if they are LU equivalent, $U \xrightarrow{\text{LU}} U'$, or not. Namely if Eq. (1) is satisfied for some local operators u_i and v_i . The problem is exacerbated for the case of 2-unitary operators as the singular values of U^R and U^T , which are LUI, are all equal, and hence maximize the standard invariants such as $E(U)$ and $E(US)$.

Here we propose a necessary criterion to investigate the LU equivalence between unitary operators based on the distributions of the entanglement they produce when applied on an ensemble of uniformly generated product states. Action of a bipartite unitary operator U on product states generically results in entangled states,

$$|\psi_{AB}\rangle = U(|\phi_A\rangle \otimes |\phi_B\rangle). \quad (78)$$

Let $\mathcal{E}(|\psi\rangle_{AB})$ be any measure of entanglement, and let ϕ_A and ϕ_B be sampled from the Haar measure on the subspaces. Then the resulting distribution $p(x;U)$ of the entanglement is

$$p(x;U) = \int \delta(x - \mathcal{E}[U(|\phi_A\rangle \otimes |\phi_B\rangle)]) d\mu(\phi_A) d\mu(\phi_B). \quad (79)$$

It is clear that if U is left multiplied by local unitaries $p(x;U)$ is unchanged as entangled measures are invariant under such operations. If $U' = U(u_A \otimes u_B)$, then $p(x;U') = p(x;U)$, as $d\mu(u_A^\dagger |\phi_A\rangle) = d\mu(|\phi_A\rangle)$, which is a property of the Haar measure. Thus if $U \xrightarrow{\text{LU}} U'$ then $p(x;U') = p(x;U)$. Conversely if $p(x;U') \neq p(x;U)$ this implies that $U \not\xrightarrow{\text{LU}} U'$.

However, if the distributions are *indistinguishable*, i.e., $p(x;U') = p(x;U)$, then U and U' *may or may not* be LU equivalent. To see that the criterion is necessary but not sufficient, consider two LU inequivalent operators U and $U' = US$, where S is the SWAP gate. Although LU inequivalent, $p(x;U) = p(x;U')$, they generate identical entanglement distributions. Note that while U and U'

have the same entangling power; $e_p(U) = e_p(U')$, but have different gate typicalities; $g_t(U) = g_t(U')$ and are thus locally inequivalent.

We enlarge local equivalence between U and U' to include multiplication by SWAP gates on either or both sides, denoted by $U' \xrightarrow{\text{LUS}} U$ as

$$U' = (u_1 \otimes v_1) S^a U S^b (u_2 \otimes v_2), \quad (80)$$

where u_i 's and v_i 's are single qudit gates, and a, b takes values 0 or 1. Any operator in the LUS equivalence class of U will produce the same entanglement distribution, $p(x;U)$.

B. 2-unitaries in $d = 3$

1. Permutations

2-unitary permutations of order d^2 maximize the entangling power and are in one-to-one correspondence with orthogonal Latin squares of size d ; OLS(d) [59]. In general, 2-unitary operators are in one-to-one correspondence with AME states of four qudits [48]. Under this mapping 2-unitary permutation matrices correspond to AME states with minimal support [48] i.e., these contain minimal possible terms equal to d^2 when written in the computational basis. A complete enumeration of all possible 2-unitary permutations of size d^2 boils down to the possible number of OLS(d) which is known for $d \leq 9$ (see A072377, Ref. [88]). For $d = 3$ there are 72 possible 2-unitary permutations of size 9. We find by a direct numerical exhaustive search over local permutation matrices of size 3 that *all* 72 possible 2-unitary permutations are LU equivalent. This observation leads to the following proposition.

Proposition 2 *There is only one LU class of 2-unitary permutations of order 9.*

We choose the following 2-unitary permutation as a representative of the LU equivalent class of 2-unitary permutations of order 9,

$$P_9 = \begin{pmatrix} 1 & \cdot \\ \cdot & \cdot \\ \cdot & \cdot \\ \cdot & \cdot \\ \cdot & \cdot \\ \cdot & \cdot \\ \cdot & \cdot \\ \cdot & \cdot \\ \cdot & \cdot \end{pmatrix} \quad (81)$$

An easy way to obtain all 72 possible 2-unitary permutations is by searching over $(3!)^4 = 1296$ local permutations p_i of size 3 in

$$P' = (p_1 \otimes p_2) P_9 (p_3 \otimes p_4). \quad (82)$$

Although this is not an efficient way as each 2-unitary permutation is repeated 18 times but all $1296/18 = 72$ possible permutations can be obtained.

An equivalent statement in terms of LU equivalence of AME(4,3) states with minimal support is known, see Ref. [60]. An AME(4,3) state with minimal support considered in Ref. [60] contains arbitrary phases and is equivalent to an emphased 2-unitary permutation *i.e.*, 2-unitary permutation multiplied by a diagonal unitary. This is a special property of 2-unitary permutations that these remain 2-unitary upon multiplication by diagonal unitaries with arbitrary phases owing to their special combinatorial structure. Indeed one can show that in $d = 3$ that all emphased permutations are LU equivalent to P_9 . Local dimension $d = 3$ is special in the sense that number of phases, $d^2 - 1 = 8$, exactly matches the number of phases one can absorb using four emphased local permutations each containing $d - 1$ phases, $4(d - 1) = 8$. Note that $d^2 - 1 = 4(d - 1)$ has a solution only for $d = 3$ and thus the above results about LU equivalence do not hold for $d > 3$.

2. LU equivalence of 2-unitaries in $d = 3$

Dynamical maps are very efficient in yielding 2-unitaries for local Hilbert space dimension $d = 3, 4$ from random seed unitaries. The 2-unitaries so obtained do not have an evident simple structure as 2-unitary permutations have. It is natural to ask if these are LU equivalent to each other. For the purposes of LU equivalence we compare the entanglement distributions of 2-unitaries obtained from the map, $p(x; U)$ with that of the 2-unitary permutation matrix $p(x; P_9)$. We find that the von Neumann entropy is a good measure to highlight the differences in the distributions, especially it performs better than the linear entropy and hence we use this. Von Neumann entropy of the single qudit reduced density matrix of $|\psi\rangle_{AB}$ (see Eq. (78)) is defined as

$$\mathcal{E}_v(\rho_A) = -\text{tr}(\rho_A \log \rho_A).$$

The distribution $p(x; P_9)$ and $p(x; U_9)$ from a 2-unitary U_9 are shown in Fig. (7). The matrix U_9 has beenb obtained using a random seed in the dynamical map $\mathcal{M}_{\Gamma R}$. Surprisingly, both the distributions are indistinguishable for these 2-unitaries, although their origins and forms are very different. We have checked entanglement distributions for $O(10^3)$ 2-unitaries obtained from the map but could not find a different distribution from that of the 2-unitary permutation matrix. In fact in most cases we could transform 2-unitaries obtained from the map, using random seeds, into 2-unitary permutation matrices using appropriate local transformations in $\mathcal{U}(3) \otimes \mathcal{U}(3)$. Based on an over-

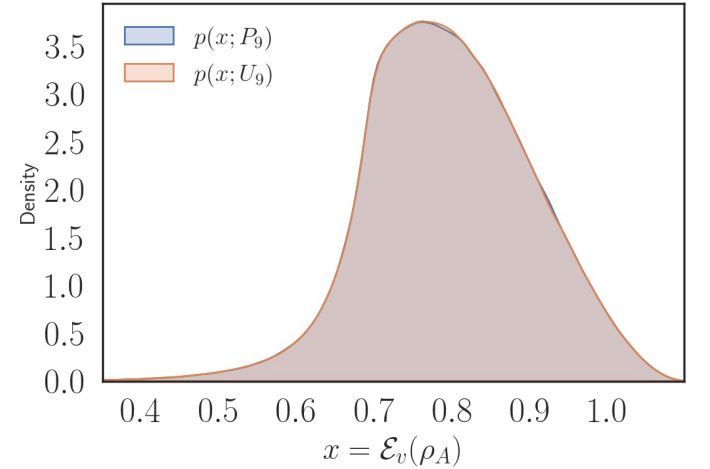


FIG. 7. Two-qutrit case, $d^2 = 9$. Distributions $p(x; U)$ of entanglement obtained from the action of 9×9 unitaries U on Haar distributed product states. Shown are two distributions, one corresponding to the 2-unitary permutation matrix P_9 , Eq. (81) and other a 2-unitary U_9 obtained from the map with a random seed. These two are numerically indistinguishable, and we could not find a different distribution than the one shown here for $O(10^3)$ number of 2-unitaries obtained from the map.

whelming numerical evidence we propose the following:

Conjecture: All 2-unitaries of order 9 are LU equivalent to P_9 .

If the above conjecture is true then all AME states of four qutrits; AME(4,3), are LU equivalent to AME(4,3) of minimal support.

C. 2-unitaries in $d = 4$

1. Permutations

The total number of 2-unitary permutations of size 16 is $2 \times 3456 = 6912$. By performing a direct exhaustive search over local permutations, quite remarkably even in this case it turns out that *all* 6912 2-unitary permutations are LU equivalent and thus lead to the following proposition.

Proposition 3 *There is only one LU class of 2-unitary permutations of order 16.*

We choose the following 2-unitary permutation matrix as a representative of the LU equivalent class of

2-unitary permutations of order 16,

$$P_{16} = \left(\begin{array}{c|c|c|c} 1 & \cdot \\ \cdot & \cdot \\ \cdot & \cdot \\ \cdot & \cdot \\ \hline \cdot & \cdot \\ \cdot & \cdot \\ \cdot & \cdot \\ \cdot & \cdot \\ \cdot & \cdot \\ \hline \cdot & \cdot \\ \cdot & \cdot \\ \cdot & \cdot \\ \cdot & \cdot \\ \hline \cdot & \cdot \\ \cdot & \cdot \\ \cdot & \cdot \\ \cdot & \cdot \end{array} \right) \quad (83)$$

Using $(4!)^4 = 3,31,776$ possible local permutations, each 2-unitary permutation is obtained 48 times and therefore all $3,31,776/48 = 6912$ are taken into account.

2. Entangled OLS of size 4: A new example of AME(4, 4)

Although there is only one LU class of 2-unitary permutations of order 16, we give an explicit example of a 2-unitary orthogonal matrix which is not LU equivalent to any 2-unitary permutation. This is obtained via the nonlinear map $\mathcal{M}_{\Gamma R}$ given in Eq. (23) with a permutation seed, and is given by

$$O_{16} = \frac{1}{2} \left(\begin{array}{c|c|c|c} 1 & \cdot & \cdot & \cdot & \cdot & 1 & \cdot \\ \cdot & 1 & \cdot & \cdot & \cdot & -1 & \cdot \\ \cdot & \cdot & -1 & \cdot & \cdot & \cdot & \cdot & \cdot & 1 & -1 & \cdot \\ \cdot & \cdot & \cdot & -1 & \cdot & \cdot & \cdot & 1 & \cdot & 1 & \cdot & \cdot & \cdot & 1 & \cdot & \cdot & \cdot \\ \hline \cdot & 1 & \cdot & \cdot & \cdot & -1 & \cdot & \cdot & \cdot & \cdot & \cdot & \cdot & 1 & \cdot & \cdot & \cdot & \cdot \\ \cdot & -1 & \cdot & \cdot & \cdot & \cdot & 1 & \cdot & \cdot & \cdot & \cdot & 1 & \cdot & \cdot & \cdot & \cdot & -1 \\ \cdot & \cdot & \cdot & -1 & \cdot & \cdot & \cdot & 1 & \cdot & \cdot & -1 & \cdot & \cdot & -1 & \cdot & \cdot & \cdot \\ \cdot & \cdot & \cdot & -1 & \cdot & \cdot & \cdot & -1 & 1 & \cdot & \cdot & \cdot & \cdot & -1 & \cdot & \cdot & \cdot \\ \hline \cdot & \cdot & \cdot & -1 & \cdot & \cdot & \cdot & -1 & -1 & \cdot & \cdot & \cdot & \cdot & \cdot & 1 & \cdot & \cdot \\ \cdot & \cdot & \cdot & 1 & \cdot & \cdot & \cdot & 1 & \cdot & -1 & \cdot & \cdot & 1 & \cdot & \cdot & \cdot & \cdot \\ \cdot & -1 & \cdot & \cdot & \cdot & \cdot & -1 & \cdot & \cdot & \cdot & -1 & \cdot & \cdot & \cdot & \cdot & -1 & \cdot \\ \cdot & -1 & \cdot & \cdot & \cdot & -1 & \cdot & \cdot & \cdot & \cdot & -1 & \cdot & \cdot & 1 & \cdot & \cdot & \cdot \\ \hline \cdot & \cdot & \cdot & -1 & \cdot & \cdot & \cdot & -1 & \cdot & -1 & \cdot & \cdot & 1 & \cdot & \cdot & \cdot & \cdot \\ \cdot & \cdot & \cdot & 1 & \cdot & \cdot & \cdot & -1 & -1 & \cdot & \cdot & \cdot & -1 & \cdot & \cdot & \cdot & \cdot \\ \cdot & 1 & \cdot & \cdot & \cdot & 1 & \cdot & \cdot & \cdot & \cdot & \cdot & -1 & \cdot & \cdot & 1 & \cdot & \cdot \\ \cdot & 1 & \cdot & \cdot & \cdot & -1 & \cdot & \cdot & \cdot & \cdot & \cdot & 1 & \cdot & \cdot & \cdot & -1 & \cdot \end{array} \right) \quad (84)$$

This matrix can be written in a compact form as

$$O_{16} = P_{16}^T D_4 P_{16}, \quad (85)$$

where D_4 is a block-diagonal matrix consisting of four 4×4 Hadamard matrices. Each row or column of O_{16} contains four non-zero entries being equal to either $1/2$ or, $-1/2$ and is such that its eighth power is equal to the Identity, $O_{16}^8 = \mathbb{I}$. To show that O_{16} is indeed not LU equivalent to P_{16} , we compare the entanglement distributions $p(x; O_{16})$ and $p(x; P_{16})$. The distributions, shown in Fig. (8) are clearly distinguishable, $p(x; O_{16}) \neq p(x; P_{16})$ and thus $O_{16} \xrightarrow{LU} P_{16}$. Entanglement distributions for a large number of generic

2-unitaries obtained by applying the dynamical map $\mathcal{M}_{\Gamma R}$ on random seed unitaries did not result in any other distinguishable distributions other than the ones shown in Fig. (8). This tentatively suggests that there are *only three* LU classes of 2-unitaries in $d = 4$, but certainly there are *at least 3* classes. The representatives of these 3 LU classes are: (i) P_{16} given by Eq. (83), (ii) enphased P_{16} ; $P'_{16} = D_1 P_{16} D_2$, where D_1 and D_2 are diagonal unitaries with arbitrary phases, and (iii) O_{16} given by Eq. (84). Note that P_{16} and P'_{16} are not LU equivalent in general and thus the corresponding AME states of minimal support are not LU equivalent.

Each row or, column of O_{16} treated as a pure state in $\mathcal{H}_4 \otimes \mathcal{H}_4$ is maximally entangled and thus the under-

lying combinatorial design corresponding to O_{16} does not factor into separable structures \mathcal{K} and \mathcal{L} defined in Eq. (70). Also note that each 4×4 block in Eq. (84) is unitary up to a scale factor and thus rows or columns of O_{16}^R are also maximally entangled states in $\mathcal{H}_4 \otimes \mathcal{H}_4$. Similar entangled combinatorial structure corresponding to 2-unitary of size 36 has been referred to as *entangled OQLS* in Ref. [55] in which entangled OQLS of size six was found. Based on our discussion in previous section on 2-unitaries of size 9 and the known fact that there are no 2-unitaries of size 4, $d = 4$ seems to be the smallest possible dimension in which entangled OLS exists.

This allows us to construct a new kind of AME state of four ququads; AME(4,4), which is not LU equivalent to AME state of minimal support constructed from P_{16} . The corresponding AME state written in computational basis is given by,

$$|\text{AME}(4,4)\rangle = \sum_{i,j,k,l=1}^4 (O_{16})_{ij,kl} |ijkl\rangle. \quad (86)$$

The tensor $T_{ijkl} = (O_{16})_{ij,kl}$ is a perfect tensor [49] whose non-zero entries are given by Eq. (84). To our knowledge this is the simplest AME state that is not derived from a classical design or is equivalent to one, for equivalence among AME states, see for example [60, 89]. Thus it qualifies as a younger cousin of the AME(4,6) which is a genuine quantum orthogonal Latin square [55]. However, unlike the golden state AME(4,6), this is purely real. Earlier constructions of ququad AME states have much larger number of particles [89].

We performed several local unitary transformations on O_{16} and reduced the number of its non-zero entries or, equivalently the support of AME state given by Eq. (86), from 64 to 42, although the transformed matrix has entries other than $\pm 1/2$.

VII. ENTANGLING PROPERTIES OF DUAL AND T-DUAL PERMUTATION MATRICES

Permutation matrices form an important class of entangling unitary operators [59]. In this section we study the entangling properties of dual and T-dual permutation matrices on $\mathcal{H}_d \otimes \mathcal{H}_d$ which are special subsets of the permutation group $P(d^2)$. Dual unitary permutation matrices have been recently explored in [90] and used as building blocks of quantum circuits with interesting dynamical behaviour [50]. Two permutation matrices P_1 and P_2 have been defined in [59] to belong to the same *entangling class* if they have the same entangling power, $e_p(P_1) = e_p(P_2)$. Two LU equivalent permutation matrices always belong to the same entangling class but permutation matrices belonging to the same entangling power need

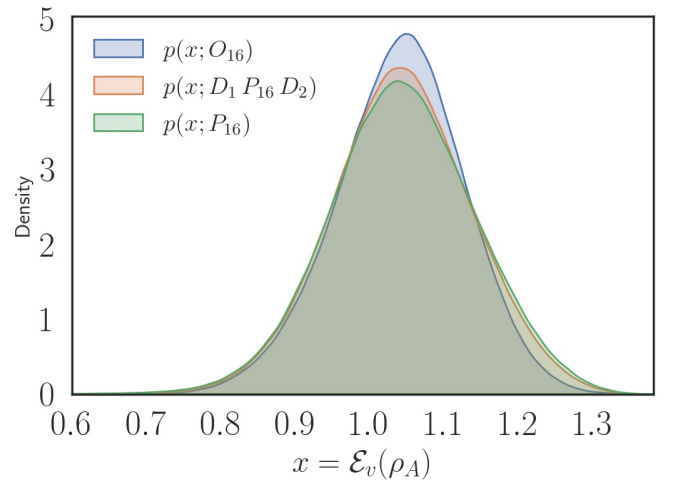


FIG. 8. Two-ququad case, $d^2 = 16$. Distributions $p(x; U)$ of entanglement corresponding to 2-unitary permutation matrix $U = P_{16}$ (Eq. (83)) and the 2-unitary orthogonal matrix $U = O_{16}$ (Eq. (84)). The distributions are clearly distinguishable and shows that P_{16} and O_{16} are not LU equivalent. Shown also is the entanglement distribution corresponding to enphased P_{16} ; $D_1 P_{16} D_2$ where D_1 and D_2 are diagonal unitaries, which is not LU equivalent to either P_{16} or O_{16} .

not be LU equivalent. For the sake of convenience we write the permutation matrix in terms of the column number of the only non-zero entry in each row. For example in this notation P_9 given by Eq. (81) is written as $P_9 = \{1, 5, 9, 6, 7, 2, 8, 3, 4\}$ corresponding to the permutation, $\pi : \{1, 2, 3, 4, 5, 6, 7, 8, 9\} \rightarrow \{\pi(1) = 1, \pi(2) = 5, \dots, \pi(8) = 3, \pi(9) = 4\}$.

A. Dual-unitary and T-dual permutations in $d = 2$ and $d = 3$

We list all possible entangling classes for dual-unitary permutations in $P(d^2)$ for $d = 2, 3$.

Two-qubit case: In this case the corresponding permutation group is $P(4)$. The projection of $P(4)$ on e_p - g_t plane is shown in Fig. (9). There are 4 distinct points corresponding to 24 possible permutations of order 4, treated as two-qubit gates, on the e_p - g_t plane and every permutation matrix is either dual or T-dual. Number of entangling classes is only 2 which are listed in Table II.

TABLE II. Entangling and LU classes of dual (equivalently T-dual) permutations in $P(4)$.

S.No.	$e_p(P)$	# LU classes
1	0	1
2	$\frac{2}{3}$	1

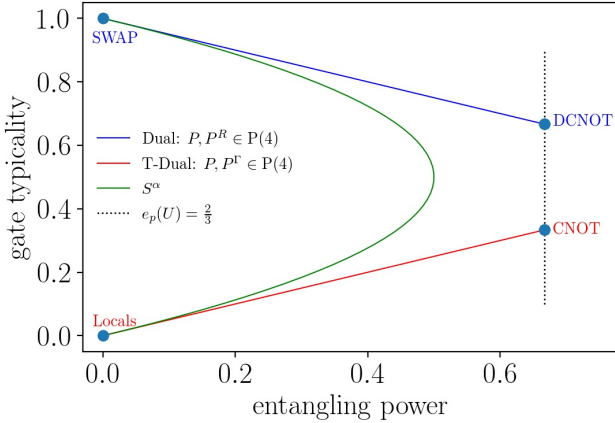


FIG. 9. Two-qubit case, $d^2 = 4$. The entangling power vs gate-typicality, of all permutations $P(4)$, treated as two-qubit gates. Number of entangling classes, those with different entangling powers, is 2.

Two-qutrit case: In this case the corresponding permutation group is $P(9)$. The projection of $P(9)$, treated as two-qutrit gates, on the e_p - g_t plane is shown in Fig. (10). There are only 60 distinct points on the e_p - g_t plane from the $9! = 3,62,000$ possible permutation matrices of order 9.

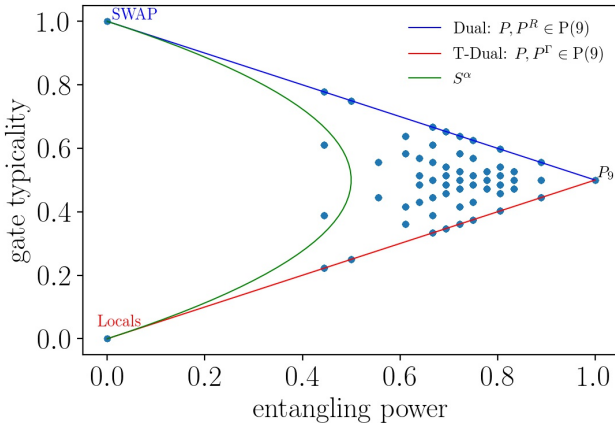


FIG. 10. Two-qutrit case, $d^2 = 9$. The entangling power vs gate-typicality, of all $9!$ permutations $P(9)$, treated as two-qutrit gates. Number of entangling classes corresponding to dual (and equivalently T-dual) permutation matrices is 10.

It was shown in Ref. [91] that there are 18 LU classes of T-dual (or equivalently dual-unitary) permutation matrices. A representative permutation from each LU class are also listed therein. These LU classes are listed in the Table III along with their entangling powers. Therefore the number of entangling classes corresponding to dual unitary (and equivalently T-dual) permutation matrices is 10.

Except for 3 entangling classes (corresponding to

TABLE III. Entangling, LU and LUS classes of dual (equivalently T-dual) permutations in $P(9)$.

S.No.	$e_p(P)$	# LU classes	# LUS classes
1	0	1	1
2	$\frac{4}{9}$	2	1
3	$\frac{1}{2}$	2	1
4	$\frac{2}{3}$	3	2
5	$\frac{25}{36}$	2	1
6	$\frac{13}{18}$	2	1
7	$\frac{3}{4}$	2	1
8	$\frac{29}{36}$	2	1
9	$\frac{8}{9}$	1	1
10	1	1	1
Total		18	11

$e_p(P) = 0, 8/9$, and 1), there are more than one LU classes. Taking permutations from two different LU classes with the same entangling power (say $e_p(P) = 1/2$), we observed that these produce the same entanglement distributions $p(x; U)$. This suggests that these LU inequivalent permutations with the same entangling power and gate typicality might be connected by the SWAP gate. Indeed we found that according to the LUS classification defined in Eq. (80) with $a = b = 1$ that there are only 11 LUS classes *i.e.*, two permutations P and P' belonging to the same entangling class but different LU classes are related (up to local permutations) as $P' = SPS$, where S is the SWAP gate. This is the case for all entangling classes in the Table III with more than one LU classes except for the entangling class $e_p(U) = 2/3$.

The entangling class $e_p(U) = 2/3$ is special and has two LUS classes. Representative permutations written in compact form as $P = \{1, 4, 8, 2, 5, 7, 6, 3, 9\}$ and $P' = \{1, 4, 9, 2, 5, 8, 6, 3, 7\}$ from both LUS classes produce distinguishable entanglement distributions shown in Fig. (11). The LU inequivalence between P and P' can also be seen via the singular values of P^Γ and P'^Γ which are LUI's (see Eq. (17)); singular values of P^Γ and P'^Γ are $\{2, 2, 1\}$ and $\{\sqrt{5}, \sqrt{2}, \sqrt{2}\}$ respectively. This leads us to the strong suspicion that the equality of entanglement distributions may be a sufficient condition for LUS equivalence, *i.e.*, $p(x; U) = p(x; U')$ iff $U \xrightarrow{\text{LUS}} U'$.

An interesting fact we observed is that with von Neumann entropy as a measure of entanglement the average of distributions obtained for these permutations differ slightly; for P , $\mathcal{E}_v(\rho_A) \approx 0.57$ while for P' , $\mathcal{E}_v(\rho_A) \approx 0.55$, taking into account 10^6 realisations of product states in both cases. Note that if the linear entropy is taken as a measure then the averages must

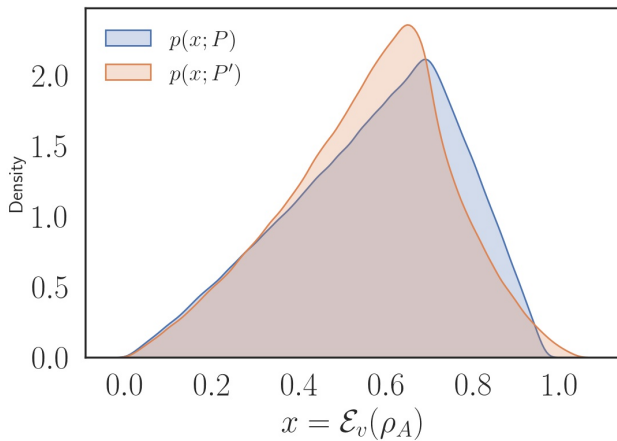


FIG. 11. Entanglement distributions obtained for P and P' permutation matrices of size 9 belonging to two LUS classes, see text, corresponding to the entangling class with $e_p(U) = 2/3$. Distinguishability of the distributions imply that P and P' are not LU equivalent.

be equal according to the definition of the entangling power [37]. This suggests the role of other unknown LU invariants besides $E(U)$ and $E(US)$ which determine the average of the entanglement distribution when von Neumann entropy is taken as a measure of entanglement.

It is to be noted that out of 18 possible LU classes *only* one corresponds to the entangling class $e_p(P) = 1$ of 2-unitary permutations. As a consequence of this all 72 possible 2-unitary permutations of order 9 are locally equivalent consistent with Proposition 2.

B. Numerical results for $d > 3$

Total possible number of LU classes of dual or, T-dual permutations in $P(d^2)$ for $d > 3$ is not known. The number of entangling classes is also not known, as an exhaustive enumeration of such permutations is prohibitively large. To get a lower bound on the possible number of entangling classes corresponding

to dual-unitary permutations of size 16 we numerically search over permutations in the vicinity of different permutations like SWAP and 2-unitary gates. Results obtained from such a search over around 1.2×10^7 permutations of size 16 (out of a possible $16! \approx 10^{13}$) is shown in Fig. (12). We obtain 56 entangling classes corresponding to dual or equivalently T-dual permutations. This provides a weak lower bound on the number of LU inequivalent classes for dual-unitary permutations of size 16. Note that one of the entangling classes is $e_p(U) = 1$ corresponding to 2-unitary permutations for which there is only one LU equivalence class (see Proposition 3).

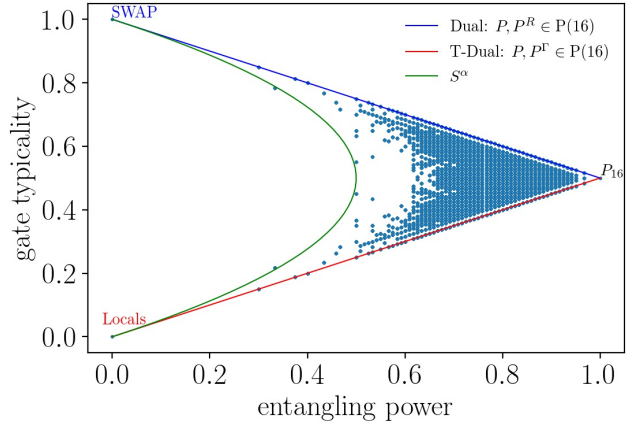


FIG. 12. Two-ququad case, $d^2 = 16$. The entangling power *vs* gate-typicality of 1.2×10^7 permutations (out of total $16! \approx 10^{13}$ permutations), treated as two-ququad gates. Number of entangling classes corresponding to dual (and equivalently T-dual) permutation matrices obtained from our numerical search is found to be 56.

We end this section by showing that there exist more than one LU classes for 2-unitary permutations in $d > 4$. An easy way to see this is by comparing entanglement distributions of 2-unitary permutation $P \in P(d^2)$ and its realignment $P^R \in P(d^2)$. This is shown in Fig. (13) for a 2-unitary permutation in $d = 5$ given by

$$P_{25} = \{1, 7, 13, 19, 25, 22, 3, 9, 15, 16, 18, 24, 5, 6, 12, 14, 20, 21, 2, 8, 10, 11, 17, 23, 4\}, \\ P_{25}^R = \{1, 7, 13, 19, 25, 8, 14, 20, 21, 2, 15, 16, 22, 3, 9, 17, 23, 4, 10, 11, 24, 5, 6, 12, 18\}. \quad (87)$$

Entanglement distributions are different; $p(x; P_{25}) \neq p(x; P_{25}^R)$ and thus establishes that they are not LU equivalent. Note that one can not justify LU inequivalence between 2-unitaries based on the singular values of their reshuffled and partially transposed re-

arrangements as they are all maximized being equal to 1. We checked entanglement distributions for 100 2-unitary permutations of size 25 together with their different rearrangements but found only two different distributions shown in Fig. (13). Thus total number of

LU and LUS classes for 2-unitary permutations in $d = 5$ remains unknown but it is certainly greater than 1. Similarly in $d = 7, 8$, and 9 we observed only two different distributions corresponding to 2-unitary permutations and their arrangements.

A consequence of having more than one LU classes of 2-unitary permutations in $d > 3$ results in minimal support AME states which are not LU equivalent. Our results thus contradict the *Conjecture 2* in Ref. [60] which in particular for four party states implies that there is only one LU class of AME states of minimal support. As we have illustrated in Fig. (8) and Fig. (13) there exist more than one LU classes of AME states of minimal support for $d = 4$ and 5.

Assuming that 2-unitary permutations belonging to the same LU class are always related by local permutations one can argue that there are more than one LU classes of 2-unitary permutations for $d = 7, 8$, and 9 as the number of possible orthogonal Latin squares (see A072377, Ref. [88]) exceeds $(d!)^4$ number of orthogonal Latin squares obtained from 2-unitary permutation P using local permutations p_i 's of size d on both sides; $(p_1 \otimes p_2)P(p_3 \otimes p_4)$. Note that all $(d!)^4$ number of orthogonal Latin squares so obtained are not all different but even with redundancy this is less than the number of possible orthogonal Latin squares in $d > 5$.

Interestingly in $d = 5$ we found that although $(d!)^4$ exceeds the number of possible orthogonal Latin squares but it is not a factor of it which is the case for $d = 3$ and 4.

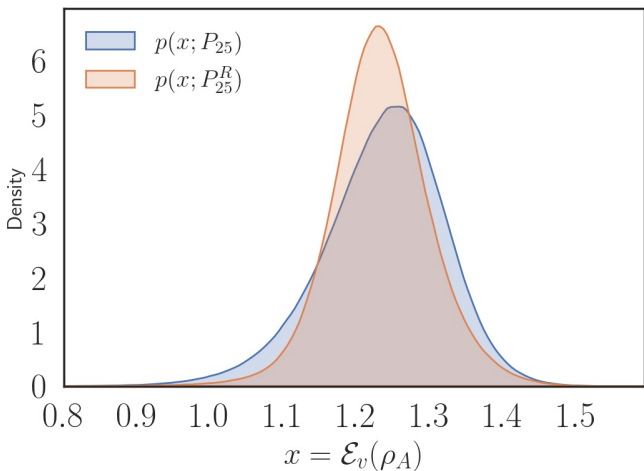


FIG. 13. $d^2 = 25$. Entanglement distributions of 2-unitary permutation P_{25} , Eq. (87), and its realignment P_{25}^R which is also a 2-unitary. The distributions are clearly distinguishable; $p(x; P_{25}) \neq p(x; P_{25}^R)$, and thus shows that $P_{25} \not\sim^{LU} P_{25}^R$.

VIII. SUMMARY AND DISCUSSIONS

Despite several constructions of the set of dual-unitary operators, the complete characterization for arbitrary local Hilbert space dimension remains an open problem. In Ref. [47], we proposed a non-linear iterative map that produces dual-unitary operators from arbitrary seed unitaries. The map acts as a dynamical system in the space of bipartite unitary operators. In this work, we have studied the period two fixed points of the map which are dual-unitary operators and provided a stochastic generalization of the map which produces structured fixed points which are dual unitaries. Complete characterization of the fixed points of all orders remains to be understood and makes the map a novel dynamical system in its own right. For two-qubit gates, using the canonical or Cartan decomposition we analytically study the convergence rates for various initial conditions. However, convergence of the map in local Hilbert space dimension $d > 2$ remains an unsolved problem.

The subset of dual-unitary operators having maximum entangling power is that of 2-unitary operators. The 2-unitary permutation operators can be constructed from combinatorial designs called orthogonal Latin squares (OLS). The non-existence of OLS of size 6 motivates to look for general quantum combinatorial designs corresponding to 2-unitary operators as was recently found in Ref. [55] for local dimension $d = 6$. The problem of finding such quantum combinatorial designs reduces to finding the 2-unitary operators which are not LU equivalent to any 2-unitary permutation matrix. From our extensive numerical searches using the dynamical map and known constructions of 2-unitaries, we could not find any such quantum design for local dimension $d = 3$. All 2-unitary permutation operators of size 9 are local unitarily (LU) equivalent to each other. Based on these results we conjecture that *all* 2-unitary operators of size 9, not just permutations, are LU equivalent to each other. If true, this implies that there is just *one* 2-unitary two-qutrit gate up to LU equivalence.

Methods to ascertain local unitary (LU) equivalence between bipartite unitary operators is not known in general. For unitary operators with identical values of known local unitary invariants (LUI's) like the entangling power and the gate typicality, the problem of LU equivalence becomes harder. In this paper we have proposed a necessary criterion for distinguishing LU inequivalent 2-unitary operators based on the entanglement distribution these produce. Using the iterative map we found a 2-unitary operator for local dimension $d = 4$ which is LU inequivalent to any 2-unitary permutation of the same size. Thus this qualifies as a genuine 2-unitary quantum design in the lowest possible dimension, as they do not exist for $d = 2$ and

as far as we know, for $d = 3$. This also implies that we have displayed an explicit example of an AME(4,4) state that is not LU equivalent to AME(4,4) of minimal support. We have shown that for $d = 5$ there are at least two LU classes of 2-unitary permutations and thus there are two LU inequivalent AME states of minimal support. Consequences of these new examples of AME states for quantum error-correction is an interesting direction and is left for future studies. Stochastic local operations and classical communication (SLOCC) equivalence of LU inequivalent four party AME states found in this work for $d > 3$ is an interesting problem and is left for future studies.

ACKNOWLEDGMENTS

We are grateful to Balázs Pozsgay for discussions on dual unitarity, and its connections to biunitarity. We thank Karol Życzkowski and Adam Burchardt for comments on a preliminary version, and for illuminating remarks on the issue of LU equivalence. Rohan Narayan and Shrigyan Brahmachari's inputs and questions were much appreciated. This work was partially funded by the Center for Quantum Information Theory in Matter and Spacetime, IIT Madras, and the Department of Science and Technology, Govt. of India, under Grant No. DST/ICPS/QuST/Theme-3/2019/Q69. SA acknowledges the Institute postdoctoral fellowship program of IIT Madras for funding during the initial stages of this work.

[1] Luigi Amico, Rosario Fazio, Andreas Osterloh, and Vlatko Vedral, "Entanglement in many-body systems," *Reviews of modern physics* **80**, 517 (2008).

[2] Bei Zeng, Xie Chen, Duan-Lu Zhou, and Xiao-Gang Wen, "Quantum information meets quantum matter—from quantum entanglement to topological phase in many-body systems," *arXiv preprint arXiv:1508.02595* (2015).

[3] Alexander Jahn and Jens Eisert, "Holographic tensor network models and quantum error correction: A topical review," *Quantum Science and Technology* (2021).

[4] Tanay Kibe, Prabha Mandayam, and Ayan Mukhopadhyay, "Holographic spacetime, black holes and quantum error correcting codes: A review," *arXiv preprint arXiv:2110.14669* (2021).

[5] Richard P Feynman, "Simulating physics with computers," in *Feynman and computation* (CRC Press, 2018) pp. 133–153.

[6] Iulia M Georgescu, Sahel Ashhab, and Franco Nori, "Quantum simulation," *Reviews of Modern Physics* **86**, 153 (2014).

[7] John Preskill, "Quantum computing in the nisq era and beyond," *Quantum* **2**, 79 (2018).

[8] Matteo Ippoliti, Kostyantyn Kechedzhi, Roderich Moessner, SL Sondhi, and Vedika Khemani, "Many-body physics in the NISQ era: quantum programming a discrete time crystal," *PRX Quantum* **2**, 030346 (2021).

[9] Frank Arute, Kunal Arya, Ryan Babbush, Dave Bacon, Joseph C Bardin, Rami Barends, Rupak Biswas, Sergio Boixo, Fernando GSL Brandao, David A Buell, *et al.*, "Quantum supremacy using a programmable superconducting processor," *Nature* **574**, 505–510 (2019).

[10] Qingling Zhu, Sirui Cao, Fusheng Chen, Ming-Cheng Chen, Xiawei Chen, Tung-Hsun Chung, Hui Deng, Yajie Du, Daojin Fan, Ming Gong, *et al.*, "Quantum computational advantage via 60-qubit 24-cycle random circuit sampling," *Science Bulletin* (2021).

[11] Adam Nahum, Sagar Vijay, and Jeongwan Haah, "Operator spreading in random unitary circuits," *Phys. Rev. X* **8**, 021014 (2018).

[12] Adam Nahum, Jonathan Ruhman, Sagar Vijay, and Jeongwan Haah, "Quantum entanglement growth under random unitary dynamics," *Physical Review X* **7**, 031016 (2017).

[13] Vedika Khemani, Ashvin Vishwanath, and David A Huse, "Operator spreading and the emergence of dissipative hydrodynamics under unitary evolution with conservation laws," *Physical Review X* **8**, 031057 (2018).

[14] CW Von Keyserlingk, Tibor Rakovszky, Frank Pollmann, and Shivaji Lal Sondhi, "Operator hydrodynamics, OTOCs, and entanglement growth in systems without conservation laws," *Physical Review X* **8**, 021013 (2018).

[15] Amos Chan, Andrea De Luca, and JT Chalker, "Solution of a minimal model for many-body quantum chaos," *Physical Review X* **8**, 041019 (2018).

[16] M Akila, D Waltner, B Gutkin, and T Guhr, "Particle-time duality in the kicked Ising spin chain," *Journal of Physics A: Mathematical and Theoretical* **49**, 375101 (2016).

[17] Bruno Bertini, Pavel Kos, and Tomaž Prosen, "Exact correlation functions for dual-unitary lattice models in 1 + 1 dimensions," *Phys. Rev. Lett.* **123**, 210601 (2019).

[18] Boris Gutkin, Petr Braun, Maram Akila, Daniel Waltner, and Thomas Guhr, "Exact local correlations in kicked chains," *Physical Review B* **102**, 174307 (2020).

[19] Petr Braun, Daniel Waltner, Maram Akila, Boris Gutkin, and Thomas Guhr, "Transition from quantum chaos to localization in spin chains," *Phys. Rev. E* **101**, 052201 (2020).

[20] Bruno Bertini, Pavel Kos, and T. Prosen, "Exact spectral form factor in a minimal model of many-body quantum chaos," *Phys. Rev. Lett.* **121**, 264101 (2018).

[21] Bruno Bertini, Pavel Kos, and Tomaž Prosen, "Entanglement spreading in a minimal model of maximal many-body quantum chaos," *Physical Review X* **9**, 021033 (2019).

[22] Bruno Bertini, Pavel Kos, and Tomaž Prosen, "Operator

entanglement in local quantum circuits i: Chaotic dual-unitary circuits," *SciPost Physics* **8**, 067 (2020).

[23] Pavel Kos, Bruno Bertini, and Tomaž Prosen, "Chaos and ergodicity in extended quantum systems with noisy driving," *Physical review letters* **126**, 190601 (2021).

[24] Alessio Leroose, Michael Sonner, and Dmitry A Abanin, "Influence matrix approach to many-body floquet dynamics," *Physical Review X* **11**, 021040 (2021).

[25] SJ Garratt and JT Chalker, "Local pairing of Feynman histories in many-body floquet models," *Physical Review X* **11**, 021051 (2021).

[26] Ana Flack, Bruno Bertini, and Tomaž Prosen, "Statistics of the spectral form factor in the self-dual kicked Ising model," *Physical Review Research* **2**, 043403 (2020).

[27] Bruno Bertini, Pavel Kos, and Tomaž Prosen, "Operator entanglement in local quantum circuits ii: Solitons in chains of qubits," *SciPost Physics* **8**, 068 (2020).

[28] Lorenzo Piroli, Bruno Bertini, J Ignacio Cirac, and Tomaž Prosen, "Exact dynamics in dual-unitary quantum circuits," *Physical Review B* **101**, 094304 (2020).

[29] Pieter W. Claeys and Austen Lamacraft, "Maximum velocity quantum circuits," *Phys. Rev. Research* **2**, 033032 (2020).

[30] Katja Klobas, Bruno Bertini, and Lorenzo Piroli, "Exact thermalization dynamics in the "rule 54" quantum cellular automaton," *Physical Review Letters* **126**, 160602 (2021).

[31] Matteo Ippoliti, Tibor Rakovszky, and Vedika Khemani, "Fractal, logarithmic, and volume-law entangled non-thermal steady states via spacetime duality," *Physical Review X* **12**, 011045 (2022).

[32] Matteo Ippoliti and Vedika Khemani, "Postselection-free entanglement dynamics via spacetime duality," *Physical Review Letters* **126**, 060501 (2021).

[33] Katja Klobas and Bruno Bertini, "Entanglement dynamics in rule 54: exact results and quasiparticle picture," *SciPost Physics* **11**, 107 (2021).

[34] Pieter W Claeys and Austen Lamacraft, "Emergent quantum state designs and biunitarity in dual-unitary circuit dynamics," *arXiv preprint arXiv:2202.12306* (2022).

[35] Tianci Zhou and Aram W. Harrow, "Maximal entanglement velocity implies dual unitarity," (2022).

[36] Paolo Zanardi, Christof Zalka, and Lara Faoro, "Entangling power of quantum evolutions," *Phys. Rev. A* **62**, 030301 (2000).

[37] Paolo Zanardi, "Entanglement of quantum evolutions," *Phys. Rev. A* **63**, 040304 (2001).

[38] Xiaoguang Wang and Paolo Zanardi, "Quantum entanglement of unitary operators on bipartite systems," *Phys. Rev. A* **66**, 044303 (2002).

[39] Xiaoguang Wang, Barry C. Sanders, and Dominic W. Berry, "Entangling power and operator entanglement in qudit systems," *Phys. Rev. A* **67**, 042323 (2003).

[40] Michael A. Nielsen, Christopher M. Dawson, Jennifer L. Dodd, Alexei Gilchrist, Duncan Mortimer, Tobias J. Osborne, Michael J. Bremner, Aram W. Harrow, and Andrew Hines, "Quantum dynamics as a physical resource," *Phys. Rev. A* **67**, 052301 (2003).

[41] G. Vidal and J. I. Cirac, "Catalysis in nonlocal quantum operations," *Phys. Rev. Lett.* **88**, 167903 (2002).

[42] K. Hammerer, G. Vidal, and J. I. Cirac, "Characterization of nonlocal gates," *Phys. Rev. A* **66**, 062321 (2002).

[43] Daniel Collins, Noah Linden, and Sandu Popescu, "Non-local content of quantum operations," *Phys. Rev. A* **64**, 032302 (2001).

[44] J. Eisert, K. Jacobs, P. Papadopoulos, and M. B. Plenio, "Optimal local implementation of nonlocal quantum gates," *Phys. Rev. A* **62**, 052317 (2000).

[45] JI Cirac, W Dür, B Kraus, and M Lewenstein, "Entangling operations and their implementation using a small amount of entanglement," *Physical review letters* **86**, 544 (2001).

[46] Mark R Dowling and Michael A Nielsen, "The geometry of quantum computation," *Quantum Information & Computation* **8**, 861–899 (2008).

[47] Suhail Ahmad Rather, S. Aravinda, and Arul Lakshminarayanan, "Creating ensembles of dual unitary and maximally entangling quantum evolutions," *Phys. Rev. Lett.* **125**, 070501 (2020).

[48] Dardo Goyeneche, Daniel Alsina, José I. Latorre, Arnau Riera, and Karol Życzkowski, "Absolutely maximally entangled states, combinatorial designs, and multiunitary matrices," *Phys. Rev. A* **92**, 032316 (2015).

[49] Fernando Pastawski, Beni Yoshida, Daniel Harlow, and John Preskill, "Holographic quantum error-correcting codes: toy models for the bulk/boundary correspondence," *Journal of High Energy Physics* **2015**, 149 (2015).

[50] S. Aravinda, Suhail Ahmad Rather, and Arul Lakshminarayanan, "From dual-unitary to quantum Bernoulli circuits: Role of the entangling power in constructing a quantum ergodic hierarchy," *Phys. Rev. Research* **3**, 043034 (2021).

[51] Jon Tyson, "Operator-schmidt decomposition of the quantum fourier transform on $n_1 \times n_2$," *Journal of Physics A: Mathematical and General* **36**, 6813–6819 (2003).

[52] Bhargavi Jonnadula, Prabha Mandayam, Karol Życzkowski, and Arul Lakshminarayanan, "Entanglement measures of bipartite quantum gates and their thermalization under arbitrary interaction strength," *Physical Review Research* **2** (2020), 10.1103/physrevresearch.2.043126.

[53] Pieter W Claeys and Austen Lamacraft, "Ergodic and nonergodic dual-unitary quantum circuits with arbitrary local hilbert space dimension," *Physical Review Letters* **126**, 100603 (2021).

[54] Satvik Singh and Ion Nechita, "Diagonal unitary and orthogonal symmetries in quantum theory ii: Evolution operators," *arXiv preprint arXiv:2112.11123* (2021).

[55] Suhail Ahmad Rather, Adam Burchardt, Wojciech Bruzda, Grzegorz Rajchel-Mieldzioć, Arul Lakshminarayanan, and Karol Życzkowski, "Thirty-six entangled officers of Euler: Quantum solution to a classically impossible problem," *Physical Review Letters* **128**, 080507 (2022).

[56] Karol Życzkowski, Wojciech Bruzda, Grzegorz Rajchel-Mieldzioć, Adam Burchardt, Suhail Ahmad Rather, and Arul Lakshminarayanan, "9 × 4 = 6 × 6: Understanding the quantum solution to the euler's problem of 36 officers," (2022).

[57] W. Helwig, W. Cui, J. I. Latorre, A. Riera, and H. K. Lo, "Absolute maximal entanglement and quantum se-

cret sharing," Phys. Rev. A **86**, 052335 (2012).

[58] Dardo Goyeneche, Zahra Raissi, Sara Di Martino, and Karol Życzkowski, "Entanglement and quantum combinatorial designs," Phys. Rev. A **97**, 062326 (2018).

[59] Lieven Clarisse, Sibasish Ghosh, Simone Severini, and Anthony Sudbery, "Entangling power of permutations," Phys. Rev. A **72**, 012314 (2005).

[60] Adam Burchardt and Zahra Raissi, "Stochastic local operations with classical communication of absolutely maximally entangled states," Phys. Rev. A **102**, 022413 (2020).

[61] Bhargavi Jonnadula, Prabha Mandayam, Karol Życzkowski, and Arul Lakshminarayanan, "Impact of local dynamics on entangling power," Physical Review A **95**, 040302 (2017).

[62] Adrian Ocneanu, "Quantized groups, string algebras and galois theory for algebras," Operator algebras and applications **2**, 119–172 (1988).

[63] Uma Krishnan and V Sunder, "On biunitary permutation matrices and some subfactors of index 9," Transactions of the American Mathematical Society **348**, 4691–4736 (1996).

[64] Vaughan FR Jones, "Planar algebras, i," arXiv preprint math/9909027 (1999).

[65] David J Reutter and Jamie Vicary, "Biunitary constructions in quantum information," arXiv preprint arXiv:1609.07775 (2016).

[66] Tristan Benoist and Ion Nechita, "On bipartite unitary matrices generating subalgebra-preserving quantum operations," Linear Algebra and its Applications **521**, 70–103 (2017).

[67] Vijay Kodiyalam, Sruthymurali, and VS Sunder, "Planar algebras, quantum information theory and subfactors," International Journal of Mathematics **31**, 2050124 (2020).

[68] Ion Nechita, Simon Schmidt, and Moritz Weber, "Sinkhorn algorithm for quantum permutation groups," Experimental Mathematics, 1–13 (2021).

[69] Boris Gutkin and Vladimir Osipov, "Classical foundations of many-particle quantum chaos," Nonlinearity **29**, 325 (2016).

[70] Ky Fan and A. J. Hoffman, "Some metric inequalities in the space of matrices," Proceedings of the American Mathematical Society **6**, 111–116 (1955).

[71] Joseph B. Keller, "Closest unitary, orthogonal and hermitian operators to a given operator," Mathematics Magazine **48**, 192–197 (1975).

[72] Tristan Benoist and Ion Nechita, "On bipartite unitary matrices generating subalgebra-preserving quantum operations," Linear Algebra and its Applications **521**, 70–103 (2017).

[73] Tomaž Prosen, "Many-body quantum chaos and dual-unitarity round-a-face?" Chaos: An Interdisciplinary Journal of Nonlinear Science **31**, 093101 (2021).

[74] N. Khaneja, R. Brockett, and S. J. Glaser, "Time optimal control in spin systems," Phys. Rev. A **63**, 032308 (2001).

[75] B. Kraus and J. I. Cirac, "Optimal creation of entanglement using a two-qubit gate," Phys. Rev. A **63**, 062309 (2001).

[76] Jun Zhang, Jiri Vala, Shankar Sastry, and K. Birgitta Whaley, "Geometric theory of nonlocal two-qubit operations," Phys. Rev. A **67**, 042313 (2003).

[77] Marcin Musz, Marek Kuś, and Karol Życzkowski, "Unitary quantum gates, perfect entanglers, and unistochastic maps," Phys. Rev. A **87**, 022111 (2013).

[78] Matthieu Vanicat, Lenart Zadnik, and Tomaž Prosen, "Integrable Trotterization: Local conservation laws and boundary driving," Phys. Rev. Lett. **121**, 030606 (2018).

[79] Antonio Mandarino, Tomasz Linowski, and Karol Życzkowski, "Bipartite unitary gates and billiard dynamics in the Weyl chamber," Phys. Rev. A **98**, 012335 (2018).

[80] Aravinda S, Suhail Ahmad Rather, and Arul Lakshminarayanan, (2020), in preparation.

[81] A Donald Keedwell and József Dénes, *Latin squares and their applications* (Elsevier, 2015).

[82] Raj Chandra Bose, Sharadchandra S Shrikhande, and Ernest T Parker, "Further results on the construction of mutually orthogonal Latin squares and the falsity of Euler's conjecture," Canadian Journal of Mathematics **12**, 189–203 (1960).

[83] Benjamin Musto and Jamie Vicary, "Quantum Latin squares and unitary error bases," Quantum Info. Comput. **16**, 1318–1332 (2016).

[84] Benjamin Musto and Jamie Vicary, "Orthogonality for quantum Latin isometry squares," Electronic Proceedings in Theoretical Computer Science **287**, 253–266 (2019).

[85] Jerzy Paczos, Marcin Wierzbniński, Grzegorz Rajchel-Mieldzioć, Adam Burchardt, and Karol Życzkowski, "Genuinely quantum solutions of the game sudoku and their cardinality," Phys. Rev. A **104**, 042423 (2021).

[86] Ion Nechita and Jordi Pillet, "Sudoq—a quantum variant of the popular game," arXiv preprint arXiv:2005.10862 (2020).

[87] Márton Borsi and Balázs Pozsgay, "Remarks on the construction and the ergodicity properties of dual unitary quantum circuits (with an appendix by Roland Bacher and Denis Serre)," arXiv preprint arXiv:2201.07768 (2022).

[88] Neil J. A. Sloane and The OEIS Foundation Inc., "The on-line encyclopedia of integer sequences," (2020).

[89] Zahra Raissi, Adam Teixidó, Christian Gogolin, and Antonio Acín, "Constructions of k -uniform and absolutely maximally entangled states beyond maximum distance codes," Phys. Rev. Research **2**, 033411 (2020).

[90] Márton Borsi and Balázs Pozsgay, "Remarks on the construction and the ergodicity properties of dual unitary quantum circuits (with an appendix by Roland Bacher and Denis Serre)," (2022), arXiv:2201.07768 [quant-ph].

[91] Uma Krishnan and Viakalathur Shankar Sunder, "On biunitary permutation matrices and some subfactors of index 9," Transactions of the American Mathematical Society **348**, 4691–4736 (1996).

[92] Albert Rico, *Absolutely maximally entangled states in small system sizes*, Ph.D. thesis, Master Thesis, Innsbruck (2020).

Appendix A: Details about the map in the two-qubit case

In two qubit computational basis, the Cartan form of any unitary (27) can be written as

$$U_0 = \begin{pmatrix} e^{-ic_3^{(0)}} c_-^{(0)} & 0 & 0 & -ie^{-ic_3^{(0)}} s_-^{(0)} \\ 0 & e^{ic_3^{(0)}} c_+^{(0)} & -ie^{ic_3^{(0)}} s_+^{(0)} & 0 \\ 0 & -ie^{ic_3^{(0)}} s_+^{(0)} & e^{ic_3^{(0)}} c_+^{(0)} & 0 \\ -ie^{-ic_3^{(0)}} s_-^{(0)} & 0 & 0 & e^{-ic_3^{(0)}} c_-^{(0)} \end{pmatrix} \quad (\text{A1})$$

where,

$$c_{\pm}^{(0)} = \cos(c_1^{(0)} \pm c_2^{(0)}), \quad s_{\pm}^{(0)} = \sin(c_1^{(0)} \pm c_2^{(0)}).$$

The unitary operator U in its canonical decomposition has four parameters. Let $\alpha_0 = e^{-ic_3^{(0)}} c_-^{(0)}$, $\beta_0 = -ie^{-ic_3^{(0)}} s_-^{(0)}$, $\gamma_0 = -ie^{ic_3^{(0)}} s_+^{(0)}$, and $\delta_0 = e^{ic_3^{(0)}} c_+^{(0)}$. Then the Eq. (A1) can be written as

$$U_0 = \begin{pmatrix} \alpha_0 & 0 & 0 & \beta_0 \\ 0 & \delta_0 & \gamma_0 & 0 \\ 0 & \gamma_0 & \delta_0 & 0 \\ \beta_0 & 0 & 0 & \alpha_0 \end{pmatrix}. \quad (\text{A2})$$

$$H = \frac{1}{2} \begin{pmatrix} |\alpha_0 - \delta_0| + |\alpha_0 + \delta_0| & 0 & 0 & -|\alpha_0 - \delta_0| + |\alpha_0 + \delta_0| \\ 0 & |\beta_0 - \gamma_0| + |\beta_0 + \gamma_0| & -|\beta_0 - \gamma_0| + |\beta_0 + \gamma_0| & 0 \\ 0 & -|\beta_0 - \gamma_0| + |\beta_0 + \gamma_0| & |\beta_0 - \gamma_0| + |\beta_0 + \gamma_0| & 0 \\ -|\alpha_0 - \delta_0| + |\alpha_0 + \delta_0| & 0 & 0 & |\alpha_0 - \delta_0| + |\alpha_0 + \delta_0| \end{pmatrix}. \quad (\text{A4})$$

The unitary $U_1 = U_0^R H^{-1}$ is given by

$$U_1 = \begin{pmatrix} \alpha_0 \alpha_+ + \delta_0 \alpha_- & 0 & 0 & \alpha_0 \alpha_- + \delta_0 \alpha_+ \\ 0 & \beta_0 \beta_+ + \gamma_0 \beta_- & \beta_0 \beta_- + \gamma_0 \beta_+ & 0 \\ 0 & \gamma_0 \beta_+ + \beta_0 \beta_- & \gamma_0 \beta_- + \beta_0 \beta_+ & 0 \\ \alpha_0 \alpha_- + \delta_0 \alpha_+ & 0 & 0 & \alpha_0 \alpha_+ + \delta_0 \alpha_- \end{pmatrix}, \quad (\text{A5})$$

where α_{\pm} and β_{\pm} are given as

$$\alpha_{\pm} = \frac{|\alpha_0 - \delta_0| \pm |\alpha_0 + \delta_0|}{2|\alpha_0 - \delta_0| |\alpha_0 + \delta_0|} \quad (\text{A6})$$

$$\beta_{\pm} = \frac{|\beta_0 - \gamma_0| \pm |\beta_0 + \gamma_0|}{2|\beta_0 - \gamma_0| |\beta_0 + \gamma_0|}$$

Note that although $U_0 \in \mathcal{SU}(4)$ but U_1 given by Eq. (A5) need not be in $\mathcal{SU}(4)$ in general. The mapping between $\alpha_0, \beta_0, \gamma_0, \delta_0$ of U_0 and $\alpha'_1, \beta'_1, \gamma'_1, \delta'_1$ of U_1

The \mathcal{M}_R map can now be studied analytically by applying it to the two qubit unitary operators in its Cartan form (A2). Action of linear map R on U_0 defined in Eq. (A2) results

$$U_0^R = \begin{pmatrix} \alpha_0 & 0 & 0 & \delta_0 \\ 0 & \beta_0 & \gamma_0 & 0 \\ 0 & \gamma_0 & \beta_0 & 0 \\ \delta_0 & 0 & 0 & \alpha_0 \end{pmatrix}. \quad (\text{A3})$$

The polar decomposition of the matrix U_0^R , which is given by $U_0^R = U_1 H$ where U_1 is unitary and $H = \sqrt{U^{R\dagger} U^R}$, and is given by

is

$$\alpha'_1 = \frac{(\alpha_0 + \delta_0)|\alpha_0 - \delta_0| + (\alpha_0 - \delta_0)|\alpha_0 + \delta_0|}{2|\alpha_0 - \delta_0| |\alpha_0 + \delta_0|}$$

$$\beta'_1 = \frac{(\alpha_0 + \delta_0)|\alpha_0 - \delta_0| - (\alpha_0 - \delta_0)|\alpha_0 + \delta_0|}{2|\alpha_0 - \delta_0| |\alpha_0 + \delta_0|}$$

$$\gamma'_1 = \frac{(\beta_0 + \gamma_0)|\beta_0 - \gamma_0| - (\beta_0 - \gamma_0)|\beta_0 + \gamma_0|}{2|\beta_0 - \gamma_0| |\beta_0 + \gamma_0|}$$

$$\delta'_1 = \frac{(\beta_0 + \gamma_0)|\beta_0 - \gamma_0| + (\beta_0 - \gamma_0)|\beta_0 + \gamma_0|}{2|\beta_0 - \gamma_0| |\beta_0 + \gamma_0|}. \quad (\text{A7})$$

The above set of equations written in a compact form

as

$$\begin{pmatrix} \alpha'_1 \\ \beta'_1 \\ \gamma'_1 \\ \delta'_1 \end{pmatrix} = \begin{pmatrix} \alpha_+ & 0 & 0 & \alpha_- \\ \alpha_- & 0 & 0 & \alpha_+ \\ 0 & \beta_- & \beta_+ & 0 \\ 0 & \beta_+ & \beta_- & 0 \end{pmatrix} \begin{pmatrix} \alpha_0 \\ \beta_0 \\ \gamma_0 \\ \delta_0 \end{pmatrix}, \quad (\text{A8})$$

depict the non-linear nature of the map.

Appendix B: Details about the map in terms of Cartan parameters

1. Map in terms of Cartan parameters

a. XXX family

For $c_1^{(n)} = c_1^{(n)} = c_1^{(n)} = c^{(n)}$, the complex number arguments appearing in Eq. (36) simplify to

$$\begin{aligned} \theta_+^{(n)} &= -\arctan \left[\frac{1 - \cos 2c^{(n)}}{1 + \cos 2c^{(n)}} \tan c^{(n)} \right], \\ \theta_-^{(n)} &= -\arctan \left[\frac{1 + \cos 2c^{(n)}}{1 - \cos 2c^{(n)}} \tan c^{(n)} \right], \\ \phi_+^{(n)} &= -\arctan \left[\frac{1}{\tan c^{(n)}} \right], \\ \phi_-^{(n)} &= \pi - \arctan \left[\frac{1}{\tan c^{(n)}} \right]. \end{aligned} \quad (\text{B1})$$

Using above equation Eq. (36) simplifies to

$$c_1^{(n+1)} = c_3^{(n+1)} = c^{(n+1)} = \frac{\pi}{4} - \frac{1}{4} \arctan \left[\frac{2}{\tan 2c^{(n)}} \right], \quad (\text{B2})$$

for all n and

$$\begin{aligned} c_2^{(n+1)} &= c^{(n+1)} \text{ for odd } n, \\ &= \frac{\pi}{2} - c^{(n+1)} \text{ for even } n \end{aligned} \quad (\text{B3})$$

where Cartan coefficients satisfy $0 \leq c_3^{(n)} \leq c_2^{(n)} \leq c_1^{(n)}$ for all n . Thus the map on Cartan parameters is 1-dimensional given by

$$c^{(n+1)} = \frac{\pi}{4} - \frac{1}{4} \arctan \left[\frac{2}{\tan 2c^{(n)}} \right]. \quad (\text{B4})$$

It is easy to check that $c^* = \pi/4$ is the fixed point of the map. We show that it is global attractor for all $c^{(0)} \in (0, \pi/4]$ below. In terms of $x_n = 1/\tan 2c^{(n)}$, Eq. (B4) becomes

$$x_n = \frac{x_{n+1}}{1 - x_{n+1}^2}, \quad (\text{B5})$$

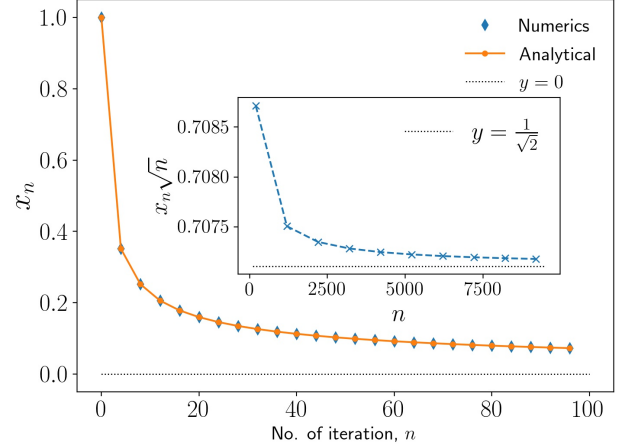


FIG. 14. XXX case: (Main) Convergence to the respective fixed point $x^* = 0$ under the map initiated with $c^{(0)} = \pi/8$, or equivalently $x_0 = 1$. (Inset) Power law behaviour for the same initial condition as seen from the convergence $x_n \sqrt{n} \rightarrow \frac{1}{\sqrt{2}}$ for large n .

which under rearrangement gives Eq. (46).

To prove convergence we write the map in terms of x_n defined in Eq. (45) as

$$\frac{x_{n+1}}{x_n} = \frac{2}{1 + \sqrt{(2x_n)^2 + 1}}. \quad (\text{B6})$$

As $1 < \sqrt{(2x_n)^2 + 1}$ for all $x_n \in (0, \infty)$. Therefore,

$$1 + \sqrt{(2x_n)^2 + 1} > 2 \implies \frac{2}{1 + \sqrt{(2x_n)^2 + 1}} < 1.$$

Hence from Eq. B6, $x_{n+1} < x_n$ and explains the contractive nature of the map. The convergence of the map can also be justified in terms of its Jacobian given by

$$J_x = \frac{d}{dx} \left[\frac{2x}{1 + \sqrt{4x^2 + 1}} \right] = \frac{2}{1 + 4x^2 + \sqrt{1 + 4x^2}},$$

with $J_x < 1 \forall x \in (0, \infty)$. The approach to the fixed point $x^* = 0$, or, equivalently the approach of U_n to the SWAP gate, is *algebraic* with exponent equal to $1/2$ as shown in Fig. (14) for $x_0 = 1$. Numerical values in Fig. (14) obtained from the algorithm proposed in [77] exactly match the analytical values obtained from Eq. (46).

b. SWAP-CNOT-DCNOT face

In this case the substitution $c_1^{(n)} = \pi/4$ and assuming $0 \leq c_3^{(n)} \leq c_2^{(n)} \leq c_1^{(n)} \leq \pi/4$, simplifies the complex number arguments in the 3-dimensional map Eq. (36)

to

$$\begin{aligned}\theta_+^{(n)} &= -\arctan \left[\tan c_2^{(n)} \tan c_3^{(n)} \right], \\ \theta_-^{(n)} &= -\arctan \left[\frac{\tan c_3^{(n)}}{\tan c_2^{(n)}} \right], \\ \phi_+^{(n)} &= -\arctan \left[\frac{1}{\tan c_2^{(n)} \tan c_3^{(n)}} \right], \\ \phi_-^{(n)} &= \pi - \arctan \left[\frac{\tan c_2^{(n)}}{\tan c_3^{(n)}} \right].\end{aligned}\quad (\text{B7})$$

Using above set of equations in Eq. (36) the map on Cartan coefficients reduces to

$$\begin{aligned}c_1^{(n+1)} &= \frac{\pi}{4}, \\ c_2^{(n+1)} &= \frac{\pi}{4} \pm \frac{1}{2} \arctan \left[\sin 2 c_3^{(n)} \cot 2 c_2^{(n)} \right], \\ c_3^{(n+1)} &= \frac{1}{2} \arctan \left[\frac{\tan 2 c_3^{(n)}}{\sin 2 c_2^{(n)}} \right].\end{aligned}\quad (\text{B8})$$

Thus the map is 2-dimensional and in terms of $y_n = 1/\tan^2 2c_2^{(n)}$ and $z_n = 1/\tan^2 2c_3^{(n)}$ the above 2-dimensional map takes a purely algebraic form given by Eq. (49) in the main text.

c. SWAP-CNOT edge

In this case the map on Cartan parameters is 1-dimensional; $c_1^{(n+1)} = \pi/4, c_2^{(n+1)} = c_3^{(n+1)} = c^{(n+1)}$, given by

$$c^{(n+1)} = \frac{1}{2} \arctan \left[\frac{1}{\cos 2 c^{(n)}} \right]. \quad (\text{B9})$$

In terms of $t_n = \tan^2(2c^{(n)})$, the above map takes a simple linear form

$$t_{n+1} = 1 + t_n, \quad (\text{B10})$$

hence $t_n = n - 1 + t_0$. In terms of $y_n = 1/\tan^2(2c^{(n)})$ reduces to Eq. (57) with exact solution given by Eq. (58). In this case the approach to the fixed point $y^* = 0$ or, equivalently the approach of U_n to the SWAP gate, is *algebraic* with exponent equal to $1/2$ as shown in Fig. (15).

Appendix C: 2-unitaries with entangled rows and columns

We write unitary operator U in block form as $U = \sum_{i,j=1}^d |i\rangle \langle j| \otimes X_{ij}$.

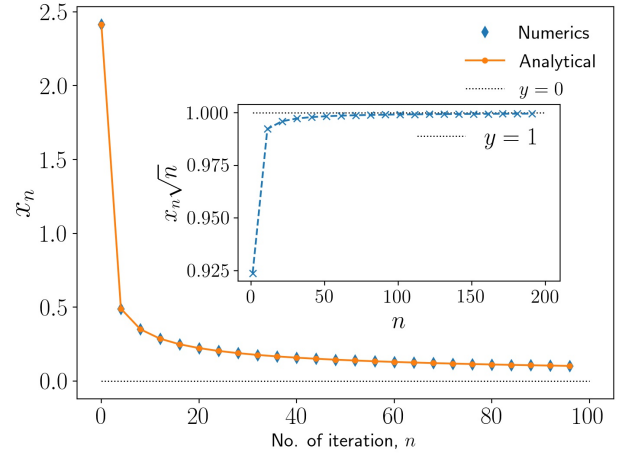


FIG. 15. SWAP-CNOT edge: (Main) Convergence to the respective fixed point $y^* = 0$ under the map initiated with $c^{(0)} = \frac{\pi}{16}$. (Inset) Power law behaviour for the same initial condition as seen from the convergence $y_n \sqrt{n} \rightarrow 1$ for large n .

1. Unitarity of U : $UU^\dagger = U^\dagger U = \mathbb{I}_{d^2}$.

$$\begin{aligned}UU^\dagger &= \left(\sum_{i,j=1}^d |i\rangle \langle j| \otimes X_{ij} \right) \left(\sum_{k,l=1}^d |k\rangle \langle l| \otimes X_{kl} \right)^\dagger, \\ &= \sum_{i,k=1}^d \left(|i\rangle \langle k| \otimes \sum_{j=1}^d X_{ij} X_{kj}^\dagger \right),\end{aligned}$$

$UU^\dagger = \mathbb{I}_{d^2}$ gives

$$\sum_{j=1}^d X_{ij} X_{kj}^\dagger = \delta_{ik} \mathbb{I}_d. \quad (\text{C1})$$

2. Dual-unitarity of U : $U^R U^{R\dagger} = U^{R\dagger} U^R = \mathbb{I}_{d^2}$.

$$\begin{aligned}U^R U^{R\dagger} &= \left(\sum_{ij} |ij\rangle \langle X_{ij}^*| \right) \left(\sum_{kl} |kl\rangle \langle X_{kl}^*| \right)^\dagger, \\ &= \sum_{ij} \sum_{kl} \langle X_{kl} | X_{ij} \rangle |ij\rangle \langle kl|,\end{aligned}$$

$U^R U^{R\dagger} = \mathbb{I}_{d^2}$ gives

$$\langle X_{kl} | X_{ij} \rangle = \delta_{ik} \delta_{jl}, \quad (\text{C2})$$

i.e, X_{ij} 's form an orthonormal operator basis.

3. T-duality of U : $U^\Gamma U^{\Gamma\dagger} = \mathbb{I}_{d^2}$.

$$\begin{aligned}U^\Gamma U^{\Gamma\dagger} &= \left(\sum_{i,j=1}^d |j\rangle \langle i| \otimes X_{ij} \right) \left(\sum_{k,l=1}^d |l\rangle \langle k| \otimes X_{kl} \right)^\dagger, \\ &= \sum_{j,l=1}^d \left(|j\rangle \langle l| \otimes \sum_{i=1}^d X_{ij} X_{il}^\dagger \right),\end{aligned}$$

$U^\Gamma U^{\Gamma\dagger} = \mathbb{I}_{d^2}$ gives

$$\sum_{i=1}^d X_{ij} X_{il}^\dagger = \delta_{jl} \mathbb{I}_d. \quad (\text{C3})$$

The above conditions are equivalent to those presented in Ref. [55] and Ref. [92] in terms of single qudit reduced density matrices (marginals) of a two-qudit pure state; $X_{ij} \mapsto |X_{ij}\rangle = (X_{ij} \otimes \mathbb{I}) |\Phi^+\rangle$. It is easy to see that the marginal with respect to the first qudit is given by $X_{ij} X_{ij}^\dagger$. Thus conditions (1) and (2) above involve orthonormality of sums of single qudit marginals in each

row and each column respectively. A $d \times d$ arrangement of d^2 -dimensional vectors (two-qudit quantum states) $|X_{ij}\rangle$ which satisfy Eqs. (C1)–(C3) form an orthogonal quantum Latin square (OQLS). This generalizes the notion of OLS for general 2-unitary operators not necessarily permutations or those for which single qudit marginals are projectors where each $|X_{ij}\rangle$ is a product state. The original definitions of OQLS [58, 84] are fragile in the sense they do not work when $|X_{ij}\rangle$ are entangled. Note that the entanglement of two-qudit states $|X_{ij}\rangle$'s change when unitary $U = \sum_{i,j=1}^d |i\rangle \langle j| \otimes X_{ij}$, is multiplied by local unitary transformations.